

Accepted Manuscript

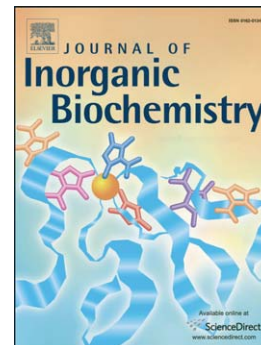
Copper(II) Complexes of Alloferon 1 with Point Mutations (H1A) and (H9A)
Stability Structure and Biological Activity

Agnieszka Matusiak, Mariola Kuczer, Elżbieta Czarniewska, Grzegorz
Rosiński, Teresa Kowalik-Jankowska

PII: S0162-0134(14)00150-0
DOI: doi: [10.1016/j.jinorgbio.2014.05.012](https://doi.org/10.1016/j.jinorgbio.2014.05.012)
Reference: JIB 9532

To appear in: *Journal of Inorganic Biochemistry*

Received date: 4 February 2014
Revised date: 22 May 2014
Accepted date: 23 May 2014



Please cite this article as: Agnieszka Matusiak, Mariola Kuczer, Elżbieta Czarniewska, Grzegorz Rosiński, Teresa Kowalik-Jankowska, Copper(II) Complexes of Alloferon 1 with Point Mutations (H1A) and (H9A) Stability Structure and Biological Activity, *Journal of Inorganic Biochemistry* (2014), doi: [10.1016/j.jinorgbio.2014.05.012](https://doi.org/10.1016/j.jinorgbio.2014.05.012)

This is a PDF file of an unedited manuscript that has been accepted for publication. As a service to our customers we are providing this early version of the manuscript. The manuscript will undergo copyediting, typesetting, and review of the resulting proof before it is published in its final form. Please note that during the production process errors may be discovered which could affect the content, and all legal disclaimers that apply to the journal pertain.

**Copper(II) Complexes of Alloferon 1 with Point Mutations (H1A) and (H9A)
Stability Structure and Biological Activity**

Agnieszka Matusiak^a, Mariola Kuczer^a, Elżbieta Czarniewska^b, Grzegorz Rosiński^b and
Teresa Kowalik-Jankowska^{a*}

^a *Faculty of Chemistry, University of Wrocław, 14 Joliot-Curie, 50-383 Wrocław (Poland)*

^b *Department of Animal Physiology and Development, Institute of Experimental Biology,
Adam Mickiewicz University, 89 Umultowska, 61-614 Poznań (Poland)*

* Corresponding author. Tel: +48 71 3757231; fax +48 71 328 23 48.

E-mail address: teresa.kowalik-jankowska@chem.uni.wroc.pl (T. Kowalik-Jankowska)

ABSTRACT

Mono- and polynuclear copper(II) complexes of the alloferon 1 with point mutations (H1A) A¹GVSGH⁶GQH⁹GVH¹²G (Allo1A) and (H9A) H¹GVSGH⁶GQA⁹GVH¹²G (Allo9A) have been studied by potentiometric, UV-visible, CD, EPR spectroscopic and mass spectrometry (MS) methods. To obtain a complete complex speciation different metal-to-ligand molar ratios ranging from 1:1 to 4:1 for Allo1A and to 3:1 for Allo9A were studied. The presence of the His residue in first position of the peptide chain changes the coordination abilities of the Allo9A peptide in comparison to that of the Allo1A. Imidazole-N3 atom of N-terminal His residue of the Allo9A peptide forms stable 6-membered chelate with the terminal amino group. Furthermore, the presence of two additional histidine residues in the Allo9A peptide (H⁶,H¹²) leads to the formation of the CuL complex with 4N {NH₂,N_{Im}-H¹,N_{Im}-H⁶,N_{Im}-H¹²} binding site in wide pH range (5-8). For the Cu(II)-Allo1A system, the results demonstrated that at physiological pH 7.4 the predominant complex the CuH₁L consists of the 3N {NH₂, N⁻,CO,N_{Im}} coordination mode. The inductions of phenoloxidase activity and apoptosis *in vivo* in *Tenebrio molitor* cells by the ligands and their copper(II) complexes at pH 7.4 were studied. The Allo1A, Allo1K peptides and their copper(II) complexes displayed the lowest haemocytotoxic activity while the most active was the Cu(II)-Allo9A complex formed at pH 7.4. The results may suggest that the N-terminal-His¹ and His⁶ residues may be more important for their proapoptotic properties in insects than those at positions 9 and 12 in the peptide chain.

Keywords: Alloferon, copper, biological activity, mono- and polynuclear complexes, apoptosis

1. Introduction

Alloferon was originally isolated from the experimentally infected insect, a blow fly *Calliphora vicina* and consists of 13 amino acids: HGVSGHGQHG VHG. It has been demonstrated that alloferon stimulates the natural cytotoxicity of human peripheral blood lymphocytes and enhances antitumor and antiviral activities through the induction of INF synthesis [1]. Lee et al. have reported that alloferon has dual functions: one is direct inhibition of the replication of Kaposi's sarcoma-associated herpesvirus and the other is effective eradication of virus-infected cells through the activation of natural killer (NK) cells [2]. Alloferon 1 monotherapy demonstrated moderate tumoristatic and tumoricidal activities comparable with low dose chemotherapy. When alloferon 1 and the cytotoxic drugs were combined in a regime of pulse immunochemotherapy the combination antitumor activity evidently exceeded that of the treatments applied individually [3]. Thus, alloferon 1 is interest as a potential anticancer drug. It was also reported that alloferon has no toxicity to normal cells and does not affect the growth of normal cells [4]. It is suggested, that alloferon might be useful as an immune-modulating reagent to increase NK cell cytotoxicity to NK-resistant human cancer cells [5]. Chernysh et al. are reported that alloferon 1 and especially its novel structural analog reffered to as allostatine are worthy of futher consideration as potential anticancer drugs [6]. Allostatin seems to be particularly perspective for adjuvant cancer immunotherapy. Since alloferon was originally identified as an anticancer reagent through the activation of the antitumor immune system, it is expected that alloferon might effectively prevent the development of skin cancer from UVB irradiation by preventing the malignant transformation of skin cells and by activating the antitumor immune systems in the skin. The preventive effect of alloferon on the development of skin cancer by UVB irradiation is under investigation [4]. In the literature is presented the opinion that the presence of a His residue in the peptide chain of a suitable structure may endow such a peptide with potent antiviral capabilities [7]. Therefore, the studies of alloferon 1 analogues modified at position 1 were performed. In these analogues the His residue at position 1 was replaced by other basic amino acid (Lys, Arg) and by the hydrophobic amino acid (Ala) [8]. The substitution of His by Ala at position 1 resulted in a complete loss of activity against studied viruses, while the replacement of His by Lys at position 1 leads to a compound with strong antiviral activity [8]. In the second group of analogues, modified at position 6 (His residue) of the alloferon peptide chain, it was found that all analogues showed the proapoptotic effect of 50 – 220 % relative to alloferon. The most active was alloferon with point mutation (H6A), Allo6A [9].

Many essential metal ions act as the important factor influencing the structure of natural and synthetic oligopeptides, and as a consequence, they may have a critical impact on their biological activity [10]. Moreover, the copper-peptide complex may be more resistant to enzymatic degradation in comparison to that of free ligand [11]. The pharmacological tests reveal that the coordination effect may improve the biological activity of the ligand [12]. Complex species are built around 4d or 5d metals: e.g. palladium and platinum [13,14], cadmium [15], gold [16], nickel(II) and copper(II) [12,17]. The activity may be also linked to the lipophilicity of the complexes: the higher the lipophilicity, the easier the penetration in the cell through the cellular membrane [18].

It was found that insect peptides as *Neb*-colloostatin [19], alloferon, and its selected analogues cause apoptosis in hemocytes of *T. molitor* [9]. Furthermore, the studies demonstrates that many Cu(II) complexes exhibit cytotoxic activity through cell apoptosis [20-23]. Also, heavy metals are known to be typical stimuli to trigger apoptosis in vertebrate and invertebrate cells [24-26]. The induction of apoptosis *in vivo* in insect cells of *Tenebrio molitor* by the alloferon mutants (H6A) and (H12A) and their copper(II) complexes at pH 7.4 was determined [27]. The biological studies show that Cu(II) ions *in vivo* did not cause any apparent apoptotic features in *T. molitor* cells but Cu(II) complexes of alloferon induce apoptosis [27]. It was also reported that Cu(II) strongly induces apoptosis *in vitro* in insect cells of *Aedes albopictus* [25].

Now, in this paper we report the synthesis of two, terminally free peptides containing three separate histidyl residues and the studies on their copper(II) complexes. The peptides involved in the study are mutants (H1A) and (H9A) of alloferon 1, H-His¹-Gly-Val-Ser-Gly-His⁶-Gly-Gln-His⁹-Gly-Val-His¹²-Gly-OH (Allo1). The peptides which are studied contain three histidine residues (H⁶,H⁹,H¹²) Allo1A (H1A) and (H¹,H⁶,H¹²) Allo9A (H9A). The copper(II) complexes were studied by the combined application of potentiometric equilibrium, spectroscopic UV-visible (UV-vis), CD and EPR and mass spectrometry methods in solution.

The induction of apoptosis *in vivo* in insect cells of *Tenebrio molitor* by the ligands studied and their copper(II) complexes at pH 7.4 was determined. Moreover, the effects of the alloferon 1, alloferon 1 mutants and their Cu(II) complexes on the phenoloxidase enzyme activity in *T. molitor* and on myocardial activity *in vitro* on the heart of *T. molitor* were studied. The coordination abilities and biological activities of the alloferon mutants (H1A) and (H9A) are compared to those of the (H6A), (H12A) [27] and (H1K) [28] analogues. The importance of the position of the His residue in the peptide chain of alloferon 1 on its biological activity is suggested.

2. Experimental

2.1. Materials

The peptides were synthesized according to a procedure reported below. As a metal ion source $\text{Cu}(\text{NO}_3)_2 \cdot 3 \text{H}_2\text{O}$ was used. KNO_3 , KOH and HNO_3 were Merck products.

2.2. Peptide syntheses, purification and characterization

Peptides were synthesized by the classical solid phase method according to the Fmoc-procedure as described previously [27,28]. Amino acids were assembled on a Fmoc-Gly-Wang resin. As a coupling reagent 2-(1H-benzotriazole-1-yl)-1,1,3,3-tetramethyluronium hexafluorophosphate (HBTU) in the presence of 1-hydroxybenzotriazole (HOBt) was used. The *N*-Fmoc (Fmoc, 9-fluorenylmethoxycarbonyl) group was removed with 20% piperidine in *N,N*-dimethylformamide (DMF). The peptide-resin was cleaved with trifluoroacetic acid (TFA) in the presence of ethanedithiol (EDT). All peptides were purified by preparative HPLC on a Varian ProStar, column -Tosoh Biosciences ODS-120T C18 (ODS 300 x 21.5 mm). Water–acetonitrile gradients containing 0.1% TFA at a flow rate of 7 ml/min were used for purification with UV detection at 210/254 nm. Analytical HPLC was performed using a Thermo Separation Products with a Vydac ProteinRP C18 column (4.6 mm × 250 mm) (Grace, Deerfield, IL, USA) with a linear gradient from 0 to 100% B in 60 min, flow rate 1 ml/min, solvent A = 0.1% TFA in water, solvent B = 0.1% TFA in 80% acetonitrile/water, UV detection at 210 nm). The molecular weights of the synthesized compounds were confirmed by ESI-MS using Apex-Qe Ultra 7T FT-ICR instrument (Bruker Daltonic, Bremen, Germany). Analytical data were as follows:

Allo1A (H1A): $R_t = 11.7$ min, $[\text{M}+\text{H}]^+$ MS = 1199.573 Da, $M_{\text{calc}} = 1199.567$ Da; $[\text{M}+2\text{H}]^{2+}$, MS = 600.295 Da, $M_{\text{calc}} = 600.287$ Da; $[\text{M}+3\text{H}]^{3+}$ MS = 400.533 Da, $M_{\text{calc}} = 400.527$ Da; Synthesis of Allo1A was carried out on a 0.25 mmol scale, yielding 280 mg (94%) dry crude peptide (74% purity). From a preparative HPLC run of 50 mg of crude Allo1A, 15 mg (30%) of pure peptide was obtained (> 98% purity).

Allo9A (H9A): $R_t = 13.0$ min, $[\text{M}+\text{H}]^+$ MS = 1199.6205 Da, $M_{\text{calc}} = 1199.567$ Da; $[\text{M}+2\text{H}]^{2+}$, MS = 600.307 Da, $M_{\text{calc}} = 600.287$ Da; $[\text{M}+3\text{H}]^{3+}$ MS = 400.531 Da, $M_{\text{calc}} = 400.527$ Da; Synthesis of Allo9A was carried out on a 0.25 mmol scale, yielding 275 mg (91%) dry crude peptide (81% purity). From a preparative HPLC run of 50 mg of crude Allo1A, 18 mg (36%) of pure peptide was obtained (> 98% purity).

Monoisotopic mass of the indicated ion formed by the peptide calculated using the mMass program.

2.3. Potentiometric measurements

Stability constants for proton and Cu(II) complexes were calculated from pH-metric titrations carried out in the argon atmosphere at 298 K using a total volume of 1.3 – 2 ml. Alkali was added from a 0.250 ml micrometer syringe which was calibrated by both weight titration and the titration of standard materials. Experimental details: ligand concentration 0.001 M for Allo1A and Allo9A, metal-to-ligand molar ratio 1:1, 2:1, 3:1 for both systems and 4:1 for Cu(II)-Allo1A (concentration of stock solution of copper(II) ions 0.05 M); the ionic strength 0.10 M (KNO₃); pH-metric titration on a MOLSPIN pH-meter system using a Russell CMAW 711 semimicro combined electrode, calibrated in concentration using HNO₃ [29]; number of titrations = 2; method of calculation SUPERQUAD [30] and HYPERQUAD [31]. The samples were titrated in the pH region 2.5 – 10.5. Standard deviations (values) quoted were computed by SUPERQUAD and HYPERQUAD and refer to random errors only. They are, however, a good indication of the importance of the particular species involved in the equilibria. The purities and exact concentration of the solutions of the ligand were determined by the method of Gran [32].

The formation reaction equilibrium of ligands with protons and copper(II) ions are given in Equation (1):



in which L are the peptides under study. The stability constant β_{pqr} is defined in Equation (2):

$$\beta_{pqr} = [\text{Cu}_p\text{H}_q\text{L}_r] / [\text{Cu}]^p \cdot [\text{H}]^q \cdot [\text{L}]^r \quad (2)$$

2.4. Spectroscopic measurements

Solutions were of similar concentrations to those used in potentiometric studies. Absorption spectra (UV-vis) were recorded on a Cary 50 “Varian” spectrophotometer in the 850 – 300 nm range. Circular dichroism (CD) spectra were recorded on a Jasco J-715 spectropolarimeter in the 750 – 250 nm range. The spectra were scanned at the pH and stoichiometric M:L values adequate to obtain the maximum formation of the particular species but also in this condition other species coexist in a smaller concentration. The values

of $\Delta\epsilon$ (i.e. $\epsilon_L - \epsilon_R$) and ϵ were calculated at the maximum concentration of the particular species obtained from potentiometric data. EPR spectra were performed in the ethylene glycol-water (1:2, v/v) solution at 77 K on a Bruker ELEXYS E 500 spectrometer equipped with NMR teslameter ER 036TM and frequency counter E 41 FC at the X-band frequency (~9.45 GHz). The spectra were analyzed by using Bruker's WIN-EPR SimFonia software, version 1.25. Copper(II) stock solution was prepared from $\text{Cu}(\text{NO}_3)_2 \cdot 3 \text{H}_2\text{O}$.

2.5. ESI-MS measurements

The mass spectra were obtained on a Bruker MicroTOF-Q spectrometer (Bruker Daltonik, Bremen, Germany), equipped with Apollo II electrospray ionization source. The mass spectrometer was operated in the positive ion mode. The instrumental parameters were as follows: scan range m/z 400–2300, dry gas - nitrogen, temperature 200 °C, reflector voltage 1300 V, detector voltage 1920 V. The samples 1:1, 2:1, 3:1 metal-to-ligand molar ratios for both systems and also 4:1 for Cu(II)-Allo1A at pH about 7 were prepared in water and infused at a flow rate of 3 $\mu\text{l}/\text{min}$. The instrument was calibrated externally with the Tunemix™ mixture (Bruker Daltonik, Germany) in quadratic regression mode.

2.6. Biological studies

Insects: A stock culture of *T. molitor* was maintained at the Department of Animal Physiology and Development as described previously [33]. Studies were carried out on 4-days old adult male beetles. As the mealworm parents' age is important for the developmental features of their offspring [34-36] all insects in our experiments derived from less than 1 month old parents. Alloferon 1, respective analogues and their copper(II) complexes were injected in MOPS buffer at pH 7.4 (Sigma-Aldrich, MOPS – 3-(*N*-morpholino)propanesulfonic acid) [37].

Phenoloxidase activity studies

The beetles were anaesthetised with CO_2 , washed in distilled water and disinfected with 70% ethanol. Alloferon or its analogue were injected (2 μl , in dose of 10 nmole per insect) through the ventral membrane between the second and the third abdominal segments towards the head with a Hamilton syringe (Hamilton Co.). The control insects were injected with the same volume of physiological saline. All peptides solutions were sterilised through the 0.22 μm pore filter membrane (Millipore) and all injections were performed in sterile

conditions. Haemolymph of control and injected insects were taken 1 h after injection for the phenoloxidase activity studies. Before haemolymph collection, the beetles were anaesthetised again with CO₂, washed in distilled water and disinfected with 70% ethanol. Upon cutting off a tarsus from a foreleg, haemolymph samples (1 µl), were collected with “end to end” microcapillaries (Drummond). Phenoloxidase activity was measured by a slight modification of the procedure described by Sorrentino et al. [38]. Briefly, 1 µl of fresh whole haemolymph samples were placed on a white filter paper (Whatman No 52) soaked in 10 mM sodium phosphate buffer (pH = 6,6) containing DL-DOPA (2 mg/ml; Sigma Aldrich). Samples were incubated for 30 min at room temperature and next, they were air-dried and scanned by CANON Lide110 (600 dpi, 8 bits, gray scale). Images were transformed, so that the darker samples correspond to the highest PO activity. Images of samples were analyzed with computer program Image J (ver. 2). The distribution of the parameters PO activity was normal, so Student’s *t*-test for paired samples was used.

In vivo haemocyte bioassay

The beetles were anaesthetised with CO₂, washed in distilled water and disinfected with 70% ethanol. Alloferon or respective analogue and Cu complexes of these peptides were injected (2 µl, in dose of 10 nmole of peptide per insect) as describes above. The control insects were injected with the same volume of physiological saline. Before haemolymph collection, the beetles were anaesthetised again with CO₂, washed in distilled water and disinfected with 70% ethanol. Both control and injected insects were taken 1 h after injection, and the haemocytes were prepared according to the method of Czarniewska et.al.[19]. The prepared haemocytes were used for the appropriate microscopic analysis (active caspase, F-actin microfilament staining and nuclei detection). The presence of active caspases was searched for by using a sulphorhodamine derivative of valylalanylaspatic acid fluoromethyl ketone, a potent inhibitor of caspase activity (SR-VAD-FMK) (in accordance to the manufacturer’s instructions of the sulphorhodamine multi-caspase activity kit, AK-115, BIOMOL, PA). Haemocytes from the control and alloferon, its analogues and Cu(II) complexes of these peptides-injected insects were allowed to adhere for 15 min. Next, they were rinsed with physiological saline, incubated in reaction medium (1/3x SR-VAD-FMK) for 1 h at room temperature in the dark, rinsed again three times with wash buffer for 5 min at room temperature and finally fixed in 3.7% paraformaldehyde for 10 min. For visualizing

F-actin microfilaments, haemocytes that first had been stained for caspase activity were permeabilized in 3.7% paraformaldehyde in physiological saline containing 0.1% Triton X-100 for 5 min at room temperature. Next, the haemocytes were washed in physiological saline and stained with Oregon Green[®] 488 phalloidin (Invitrogen) for 20 min at room temperature in the dark, in accordance to the manufacturer's instructions. After washing again in physiological saline, the haemocytes were stained with freshly prepared solutions of DAPI (Sigma) in physiological saline. Incubation in the dark lasted for 5 min. Thereafter, the haemocytes were washed once with distilled water, they were mounted using a mounting medium, and examined with a Nikon Eclipse TE 2000-U fluorescence microscope. The intensity of the apoptosing cells was measured by using NIS-Element AR 3.1 programme. The changes in fluorescence intensity were used to quantify the activity of caspases. Data are shown as mean \pm SD. The percentage of apoptotic was calculated as apoptotic haemocytes to total haemocytes in each ($[\text{number of fluorescent apoptotic cells}/\text{number all cells}] \times 100\%$).

In vitro semi-isolated heart bioassay

In order to determination influence on myocardial activity of alloferon, its analogues and their copper(II) complexes, the microdensitometric method described by Rosiński and Gade was used [39]. All experiments were carried out on semi-isolated heart of one-month old adults of the beetle *T. molitor*. After anaesthesia insects were decapitated and the legs, elytra and wings were removed. For heart preparation only abdomen was used. With surgical tools the sclerotized ventral part of cuticle was removed by cutting it along the abdomen about 1 mm from lateral part of it. Only the last segment of the sclerotized cuticle was left. Finally fat body, gut and reproductive organs were removed. During the preparation and after it, the isolated heart was washed by saline solution. Semi-isolated heart was placed in incubation chamber and continuously perfused by saline solution for 15 min to return it to the basic heart beating rhythm. For myocardial activity recording, the computer program LARWA (designed in our Lab) was used. The tested compounds were applied in 10 μ l volume at concentration 0.1 μ M and 10 μ M to application port of microperfusion system. Changes in the frequency and amplitude contractions of heart were recorded with computer programme ANALIZA (designed in our lab.). Changes in the heart contractions are presented. Changes were as ratio of average frequency of control (30 s before application of tested compounds) to average frequency after application of tested compounds (during 30 s after application). For statistical

analysis one-way ANOVA (analysis of variance) conjugated with Tukey's range test was used.

3. Results and Discussion

3.1. Protonation constants of the Allo1A (H1A) and Allo9A (H9A)

Protonation constants of the alloferon 1 mutants have been determined by potentiometric titrations, and the data are included in Table 1. The ligands show five proton-accepting centers, as expected. The amino group is the most basic center of the peptides studied. The $\log K$ value of the N-terminal amino-group depends on the nature of the N-terminal amino acid. The imidazole side chain on the His residue makes the amino group of the peptide more acidic in comparison to those of Gly-Gly-His [40]. The amino group $\log K$ values of the peptides studied are similar to those of the peptides containing His [41-42] or Ala [43-45] residues at the N-terminal position. The molecules of the peptides contain three histidyl residues, namely His¹, His⁶ and His¹² for Allo9A (H9A) and His⁶, His⁹ and His¹² for Allo1A (H1A). Deprotonations of the protonated imidazolium side chains take place in the pH range from 5 to 7, with the average values changing from (pK values) 6.14 to 6.43 (Table 1). The small differences in the pK values of the two ligands suggest that the deprotonation of the imidazolium groups completely overlaps. As a consequence, the stepwise constants cannot be assigned to specific histidyl residues and data can only be considered to be simple macroscopic thermodynamic parameters. The other protonation constants concern the C-terminal carboxyl group with the stepwise value ($\log K$) below 3.5 (Table 1) [45]. It should be mentioned, that the -Gly¹⁰-Val-His¹²-Gly-OH fragment of the peptides studied here ($\log K$ 3.16 and 3.14) is the same as for the alloferon 1 (3.19) [46], and $\log K$ values of the C-terminal carboxyl groups are similar to each other.

3.2. Equilibria analysis of the Cu(II) complexes

The stability constants of the copper(II) complexes of the Allo1A and Allo9A have been determined by potentiometric titrations by using three (Allo9A) and four (Allo1A) different metal-to-ligand molar ratios (M/L 4:1 for Allo1A, and 3:1, 2:1 and 1:1 for both peptides). For the systems studied, the precipitation of copper(II) hydroxide was never observed at any M/L ratios or pH values; this suggests the formation of mono-, bi-, tri-, and

tetranuclear complexes. In the case of the Allo9A the histidyl residues in positions H¹, H⁶, H¹² may form trinuclear Cu(II) complexes while the Allo1A contain three histidyl residues H⁶, H⁹, H¹² and N-terminal amino group, therefore, the formation of tetranuclear complexes is possible. The stability constants of different species can be calculated in the Cu(II)-Allo9A or Cu(II)-Allo1A systems (Table 1), but it requires the use of the HYPERQUAD computer program [31]. To check and/or modify the computational models all possible spectroscopic methods for paramagnetic Cu(II) complexes were applied. UV-vis and EPR spectroscopies were used to get complementary information about the number of coordinated nitrogen atoms as well as the geometry of the copper(II) complexes. CD spectra helped us to differentiate between the different types of nitrogen atoms that participate in metal coordination. Electrospray ionization mass spectrometry (ESI-MS) measurements aided the interpretation of the equilibria data by confirming the stoichiometry and binding sites of the metal complex formed. All spectroscopic data suggest that the amine N-terminal group and the imidazole residues of the peptides behave as independent metal-binding sites. The best fitting of the potentiometric data was obtained by invoking the species listed in Table 1.

3.3. Mononuclear Cu(II) complexes of the Allo1A and Allo9A peptides

For the Cu(II)-Allo1A system computer analysis of the potentiometric data has revealed the presence eight mononuclear complexes: CuH₃L, CuH₂L, CuHL, CuL, CuH₁L, CuH₂L, CuH₃L and CuH₄L (charges omitted for simplicity, Figure 1a, Table 1). Figure 1a shows that the existence of the CuHL, CuL, CuH₁L, CuH₂L and CuH₄L species is characteristic in the samples containing a 1:1 metal-to-ligand molar ratio. The spectroscopic and magnetic parameters calculated from the EPR spectra of frozen solutions are listed in Table 2. For the Cu(II)-Allo1A 1:1 molar ratio system species distribution of the complexes formed as a function of pH is similar to that of the Cu(II)-AlloK 1:1 system [28]. Moreover, the spectroscopic data for both systems are also similar to each other. The logK* value ($\log K^* = \log \beta(\text{CuH}_j\text{L}) - \log \beta(\text{H}_n\text{L})$ where the index *j* corresponds to the number of the protons in the coordinated ligand to metal ion and *n* corresponds to the number of protons coordinated to ligand) of the CuHL complex (-10.50) of the Allo1A with the 3N {NH₂,CO,2N_{im}} coordination mode is similar to that of the CuH(LH) species of the Allo1K (-10.62) [28] with similar binding sites. This similarity of the logK* for the CuHL (Allo1A) and CuH(LH) (Allo1K) complexes may suggest the coordination of the histidine residues with the formation of the macrochelate with similar size ring: (H⁶,H⁹), or (H⁶,H¹²), or (H⁹,H¹²). The EPR parameters for the CuHL complex *g*=2.275 and A_{II}=158 G, and *d-d* transition energy at 628

nm (Figure S1), compared to that provided by the equation of Prenesti [47] ($\lambda_{\max}=626$ nm) correspond to the 3N $\{\text{NH}_2, \text{CO}, 2\text{N}_{\text{Im}}\}$ binding site (Table 2). The low value of A_{II} (158 G, Table 2) may reflect deformation of the complex plane expected when a macrochelate ring is formed. The low values of A_{II} were observed for complexes containing the macrochelate formed by the histidine residues [48]. The first amide nitrogen deprotonation is slightly suppressed (6.69, Table 1) in comparison to that of Gly₅His (5.48) [48], but is compared to that of the Allo1K (6.93) [28]. At physiological pH 7.4 the CuH₁L complex dominates with 3N $\{\text{NH}_2, \text{N}^-, \text{CO}, \text{N}_{\text{Im}}\}$ or 4N $\{\text{NH}_2, \text{N}^-, 2\text{N}_{\text{Im}}\}$ coordination modes. The energy of *d-d* transition at 607 nm (Table 2, Figure S1) compared to that provided by the equation of Prenesti [47] for the 3N $\{\text{NH}_2, \text{N}^-, \text{CO}, \text{N}_{\text{Im}}\}$ λ_{\max} 599 nm suggests rather the 3N binding site than 4N (556 nm from equation of Prenesti) for the CuH₁L complex. The amine and amide nitrogen atoms from N-terminal part of the Allo1A peptide beside the imidazole nitrogen atom of histidine residue H⁶, H⁹ or H¹² are coordinated to copper(II) ions. Therefore, the coordination isomers are likely for the CuH₁L complex. With increasing pH above 7.5 the shift of the *d-d* transition energy to higher values ($\lambda_{\max}=559$ nm, Table 2) indicates deprotonation and coordination of subsequent amide nitrogens. At pH above 8 the CuH₃L and CuH₄L complexes are present in solution with the same 4N $\{\text{NH}_2, 3\text{N}^-\}$ or 4N $\{\text{N}_{\text{Im}}, 3\text{N}^-\}$ coordination modes. The spectroscopic parameters obtained at pH 9.5 – 10.5 are similar to each other (Table 2). It is reported that the terminal amino group is a more effective anchor for amide coordination than the side chain imidazole [49]. Therefore, it is likely that for the CuH₃L and CuH₄L complexes the 4N $\{\text{NH}_2, 3\text{N}^-\}$ binding site is present (Figure S2). For the CuH₃L complex of Allo1A peptide log*K** value (-20.51, Table 1) is similar to that of the Allo1K (-20.91) [28] suggesting no effect of the first amino acid residue (A,K) on the stability constant value.

The ESI-MS spectra obtained for the Cu(II)-Allo1A 1:1 metal-to-ligand molar ratio system recorded in the positive mode show dominant signals for the mononuclear complexes: [CuHL]³⁺ (420.8 Da), [CuL]²⁺ (631.2 Da, Figure S3) and [CuH₁L]⁺ (1260.5 Da) supporting the formation of the mononuclear complexes in the MS experimental conditions. The ESI-MS method has been used in a wide variety of fields to study the formation, stoichiometry, and speciation of metal complexes of organic ligands [50-52].

The stability of the complexes formed in the Cu(II)-Allo9A system was determined by analysis of the potentiometric studies carried out at 1:1, 2:1 and 3:1 metal-to-ligand molar ratios. The best model with the stoichiometries (charges have been omitted for clarity) reported in Table 1 was chosen. From potentiometric data calculations eight mononuclear complexes are found for the Cu(II)-Allo9A system (Table 1, Figure 1b). In solution

containing a 1:1 metal-to-ligand molar ratio, the following species are present: CuH_3L , CuH_2L , CuHL , CuL , CuH_{-1}L , CuH_{-3}L , CuH_{-4}L and CuL_2 . Omission of the CuL_2 species from the Cu(II)-Allo9A equilibria caused a deterioration in the goodness of fit between experimental and measured pH values in the pH range 7 – 9.5. The stability constant of the CuL_2 complex (18.12,

le 1) is compared to that obtained for the CuL_2 species of the Cu(II)-His system (17.99) [53] suggesting the same $4\text{N } 2 \times 2\text{N}\{\text{NH}_2, \text{N}_{\text{Im}}\text{-His}^1\}$ binding sites of Allo9A to copper(II) ions. At low pH, three protonated complexes CuH_3L , CuH_2L and CuHL are formed in a strongly overlapping manner. The EPR data $A_{\text{II}}=158 \text{ G}$, $g_{\text{II}}=2.285$ (Table 3) at pH=4 and low intensity CD spectrum reflect mostly to the binding mode in the dominating the CuH_2L species, and suggest histamine-like $\{\text{NH}_2, \text{N}_{\text{Im}}\text{-H}^1\}$ coordination mode. The next deprotonations result in characteristic changes on the UV-vis and EPR spectra, indicating the increase of the ligand-field strength around the metal ion. The subsequent deprotonations $\text{CuH}_2\text{L} \rightarrow \text{CuHL} \rightarrow \text{CuL}$ with pK values 4.46 and 5.10 (Table 1) correspond very well to the deprotonation and coordination of the imidazole nitrogen atoms to the copper(II) ions. Between pH 4.5 and 8.5 the CuL complex is the dominant species in the solution. Lack of the $d-d$ transitions in CD spectra for the complexes formed in the 3.5 – 8.5 pH range may support coordination of the imidazole nitrogen of the histidine residues rather than amide nitrogens (Table 3) [54,55]. This is indirect proof for coordination of the metal ion by the side chain histidine residues, which are rather far from the chirality centers of the molecule. In CuL species low value of $A_{\text{II}} = 180 \text{ G}$, $g_{\text{II}} = 2.250$ (Figure S4), and the $d-d$ transition energy at 598 nm compared to that provided by the equation of Prenesti [47], ($\lambda_{\text{max}}=577 \text{ nm}$) may be explained by the distortion of the coordination geometry of copper(II) caused by the formation of a macrochelates. The thermodynamic stability of this species for Allo9A $\log\beta(\text{CuL}) = 12.57$ (Table 1) is comparable to those of the Allo6A (12.33) [28] and alloferon 1 (12.60) [46]. It means that it is likely that alloferon 1 may coordinate copper(II) ions in the CuL complex by amine and imidazole H^1 , H^6 , H^{12} and/or H^1 , H^9 , H^{12} nitrogen atoms. The coordination isomers cannot be excluded (Figure 2). The formation of the Cu_2L_2 complex is also likely (Figure 2c). Although, the EPR spectra indicate rather the formation of mononuclear complex than dimer. Moreover, if two copper(II) ions in dimeric species are located far from each other, the monomeric spectrum will be also seen. It should be mentioned that His-rich N-terminal metal binding domain from *Haemophilus ducreyi* ($\text{H}^1\text{GDH}^4\text{MH}^6\text{NH}^8\text{DTK}$) forms also $4\text{N}\{\text{NH}_2, 3\text{N}_{\text{Im}}\}$ complex with lower stability constant (11.73) by about 0.8 log units compared to that of Allo9A [56]. At physiological pH (7.4) the CuL complex with $4\text{N}\{\text{NH}_2, \text{N}_{\text{Im}}\text{-H}^1, 2\text{N}_{\text{Im}}\}$

coordination mode dominates. The 4N coordination mode in CuL species is supported by the presence of nine superhyperfine lines in EPR spectra for the Cu(II)-Allo9A 1:1 metal-to-ligand molar ratio at pH 6.5 (Figure S4). The deprotonation and coordination of first amide nitrogen occurs with pK value 7.77 in comparison to that of the HSDGI-NH₂ equals to 6.35 [57]. It is the second proof for the 4N binding sites in the CuL species. It is known that imidazole-N3 atom of N-terminal His residue (Allo6A, Allo9A and Allo12A) can form stable 6-membered chelate with the terminal amino group. This interaction significantly enhances the thermodynamic stability of simple mono- and bis(ligand) complexes and suppresses amide deprotonation [49]. For the Cu(II)-Allo6A, Cu(II)-Allo9A and Cu(II)-Allo12A systems the formation of the CuL complex with 4N {NH₂,N_{im}-H¹,2N_{im}} coordination mode suppresses the amide deprotonation to pH above 7.5. The Allo6A, Allo9A and Allo12A form the CuL complex with similar 4N {NH₂,N_{im}-H¹,2N_{im}} binding modes but different coordination isomers. The stabilities of the macrochelates follow the order Allo9A (H¹,H⁶,H¹²)(12.57) ~ Allo6A (H¹,H⁹,H¹²)(12.33) > Allo12A (H¹,H⁶,H⁹) (10.90). With increasing pH above 7.5 the *d-d* transition energy is shifted to higher values indicating a stronger ligand field around copper(II) ion resulting from the coordination of amide nitrogens to the metal ion in the equatorial plane. For the CuH₃L and CuH₄L complexes the magnetic parameters $g_{II} = 2.218$ and $A_{II} = 192$ G are characteristic of a 4N complex species with a {NH₂,3N⁻} or {N_{im},3N⁻} binding mode (Figure S4). The absorption maximum at $\lambda_{max} = 550$ nm (Table 3) suggests a weak axial interaction (most likely) of the imidazole side chain of the histidine residue. For the CuH₃L complexes of Allo6A the *d-d* transition energy was observed at 525 nm [27], while for the Allo12A similar to that of Allo9A (550 nm) at 547 nm. If in pH above 9 the 4N {NH₂,3N⁻} complex is formed, the similarities of the *d-d* transition energy of the Cu(II)-Allo9A and Cu(II)-Allo12A systems may suggest the axial coordination of the His⁶ residue to the copper(II) ions. Above pH 10 the CuH₄L complex is present in solution. The pK value (10.12, Table 1) for the reaction $CuH_3L \rightarrow CuH_4L + H^+$ suggests: 1) the deprotonation and coordination of the amide nitrogen atom, 2) water hydrolysis, or 3) deprotonation of the pyrrole-type N(1)H group of the coordinated imidazole ring of the histidine residue, which can lead to the formation of imidazolato-bridged polynuclear species [58]. However, the parameters of UV-vis, CD and EPR spectra are not altered in solution above pH 9.5 suggesting the same binding mode in both CuH₃L and CuH₄L complexes. Therefore, the formation of the CuH₄L species may be assigned to the deprotonation of the N(1)-pyrrolic nitrogen in the imidazole ring without metal coordination [59].

The ESI-MS spectra obtained for the Cu(II)-Allo9A 1:1 metal-to-ligand molar ratio system recorded in the positive mode show dominant molecular ions: $[\text{CuHL}]^{3+}$ (420.8 Da), $[\text{CuL}]^{2+}$ (630.8 Da) and $[\text{CuH}_1\text{L}]^+$ (1260.6 Da) supporting the formation of the mononuclear complexes in the MS experimental conditions.

It should be mentioned that in equimolar solutions the dinuclear complexes are formed in the range 5 – 20% (Figures 1a and 1b). For the Cu(II)-Allo1A 1:1 system the dimeric $\text{Cu}_2\text{H}_1\text{L}$ species is present in 5% at pH about 5.5, while for the Cu(II)-Allo9A (like to Allo6A and Allo12A) the dimeric species are present at pH above 7.5.

3.4. Dinuclear complexes of Allo1A and Allo9A

For the Allo1A, monodentate binding of independent amine and histidines through the N_{Im} -donor atoms should have the $\text{Cu}_2\text{H}_2\text{L}$ stoichiometry, but stability constants can be calculated only for $\text{Cu}_2\text{H}_1\text{L}$ and the less protonated counterparts. It can be explained by the preference of the N_{Im} atoms for macrochelation. The major species among the dinuclear complexes of the Allo1A are $\text{Cu}_2\text{H}_5\text{L}$ and $\text{Cu}_2\text{H}_7\text{L}$ (Figure 3a). The $\text{Cu}_2\text{H}_5\text{L}$ species predominates around pH 8.5 – 9.0, and the stoichiometry and spectral parameters suggest the $4\text{N} \{ \text{NH}_2, 3\text{N}^- \} 4\text{N} \{ \text{N}_{\text{Im}}, 2\text{N}^-, \text{N}_{\text{Im}} \}$ coordination mode. In UV-vis, the $d-d$ transition energy at 582 nm, in CD spectra of the $\text{N}_{\text{Im}} \rightarrow \text{Cu(II)}$ at 342 nm [60] and $\text{N}(\text{amide}) \rightarrow \text{Cu(II)}$ at 307 nm charge transfer transitions (Table 2), and the broad EPR spectra with parameters $A_{\text{II}}=200$ G, $g_{\text{II}}=2.195$ are consistent with suggested binding sites for the $\text{Cu}_2\text{H}_5\text{L}$ species. The equatorial arrangement of the donors in the species $\text{Cu}_2\text{H}_5\text{L}$ includes likely $4\text{N} \{ \text{NH}_2, 3\text{N}^- \}$ (517 nm obtained from equation of Prenesti [47]) and $4\text{N} \{ \text{N}_{\text{Im}}, 2\text{N}^-, \text{N}_{\text{Im}} \}$ (542 nm) binding sites. A red shift of the $d-d$ energy band (582 nm) may result from the axial interaction of the imidazole nitrogen atom of His residue [61]. Further, two deprotonation reactions take place around pH 9 (pK 9.67 and 9.88) and these are accompanied with the blue shift of the $d-d$ of the energy band to 556 nm (Table 2). The stoichiometry and all spectral parameters are characteristic of those reported for the 4N complex of the Cu(II)-Allo1A system. The parameters of UV-vis, CD and EPR spectra are not altered in basic solution (pH 10 – 11 range) suggesting the same binding sites in the $\text{Cu}_2\text{H}_6\text{L}$ and $\text{Cu}_2\text{H}_7\text{L}$ complexes (Figure 3a). Therefore, the formation of the $\text{Cu}_2\text{H}_7\text{L}$ species can be assigned to the further deprotonation of the N(1)-pyrrolic nitrogen in the imidazole ring without metal coordination [59]. The difference in the distribution diagrams of the complexes for the Cu(II)-Allo1A and Cu(II)-Allo1K 2:1 metal-to-ligand molar ratio [28] is in pH range above 7.5. For the Allo1K the $\text{Cu}_2\text{H}_3\text{L}$ ($\text{Cu}_2\text{H}_4(\text{LH})$)

species) complex is dominant while for the Cu(II)-Allo1A the $\text{Cu}_2\text{H}_5\text{L}$. It may result from the preference of these peptides to different coordination isomers.

Two dinuclear complexes are the major species in the Cu(II)-Allo9A 2:1 metal-to-ligand molar ratio system (Figure 3b). The $\text{Cu}_2\text{H}_5\text{L}$ complex dominates in the pH range 7.5 – 10.0, whereas at higher pH values $\text{Cu}_2\text{H}_7\text{L}$ species is formed. It should be mentioned that for 2:1 molar ratio system of the Cu(II)-Allo6A the $\text{Cu}_2\text{H}_3\text{L}$ and $\text{Cu}_2\text{H}_7\text{L}$ species dominate while for the Cu(II)-Allo12A the $\text{Cu}_2\text{H}_2\text{L}$, $\text{Cu}_2\text{H}_4\text{L}$ and $\text{Cu}_2\text{H}_6\text{L}$ complexes [27]. The deprotonation constant values and coordination of the amide nitrogen atoms to copper(II) ions for the Allo9A are lower in comparison to those of Allo6A and Allo12A (Table 1) [27]. These differences result from different amino acid residues in the peptide chain near the His residues involved in the binding of the copper(II) ions (coordination isomers). The stoichiometry of the $\text{Cu}_2\text{H}_5\text{L}$ complex and the spectroscopic parameters of UV-vis, CD and EPR spectra may suggest the $4\text{N} \{ \text{NH}_2, 3\text{N}^- \}$ $4\text{N} \{ \text{N}_{\text{Im}}, 2\text{N}^-, \text{N}_{\text{Im}} \}$ binding modes around two metal ions (Table 3, Figure S5). With increasing pH the $\text{Cu}_2\text{H}_5\text{L}$ complex lost protons and the $\text{Cu}_2\text{H}_6\text{L}$ and the $\text{Cu}_2\text{H}_7\text{L}$ species are formed (Figure 3b). The $\log K^*$ values of the Cu(II)-Allo9A (-40.86, Table 1), Cu(II)-Allo6A (-43.86) and Cu(II)-Allo12A (-44.66) systems suggest higher stability of the $\text{Cu}_2\text{H}_6\text{L}$ complex of the Allo9A peptide in comparison to those of the Allo6A and Allo12A [27]. For the $\text{Cu}_2\text{H}_6\text{L}$ and $\text{Cu}_2\text{H}_7\text{L}$ complexes, the spectroscopic parameters suggest the same $4\text{N} \{ \text{NH}_2, 3\text{N}^- \}$ $4\text{N} \{ \text{N}_{\text{Im}}, 3\text{N}^- \}$ coordination modes (Table 3). In these complexes only one imidazole nitrogen atom of histidine residue is coordinated from three present in the molecule, therefore, the coordination isomers cannot be excluded [62]. The presence of the coordination isomers and the difference in the ratio of these isomers are well seen in the difference of the speciation of these Cu(II)-Allo9A, Cu(II)-Allo6A and Cu(II)-Allo12A 2:1 metal-to-ligand molar ratio systems [27].

The ESI-MS spectra obtained for the Cu(II)-Allo1A 2:1 metal-to-ligand molar ratio system recorded in the positive mode show dominant molecular ions: $[\text{Cu}_2\text{H}_1\text{L}]^{3+}$ (441.8 Da); $[\text{Cu}_2\text{H}_2\text{L}]^{2+}$ (661.2 Da, Figure 4); $[\text{Cu}_2\text{H}_3\text{L}]^+$ (1321.4 Da), while in MS spectra for the Cu(II)-Allo9A system only one molecular ion $[\text{Cu}_2\text{H}_2\text{L}]^{+2}$ (661.2 Da) was observed.

3.5. Trinuclear complexes of Allo1A and Allo9A

As it is seen for the Cu(II)-Allo1A 3:1 metal-to-ligand molar ratio system (Figure 5a) the $\text{Cu}_3\text{H}_7\text{L}$ complex is dominant in pH range 6.5 – 9.5. The stoichiometry may suggest likely coordination modes the $4\text{N} \{ \text{NH}_2, 3\text{N}^- \}$ (predicted value from equation of Prenesti 517 nm, [47]) $4\text{N} \{ \text{N}_{\text{Im}}, 2\text{N}^-, \text{N}_{\text{Im}} \}$ (542 nm) $3\text{N} \{ \text{N}_{\text{Im}}, 2\text{N}^- \}$ (584 nm) although the λ_{max} value is equal

613 nm. This red shifted of the *d-d* transition in comparison to those predicted indicates the distortion of square planar coordination geometry around the metal ions [61]. Distorted D_{4h} geometry around the copper(II) ions is also seen in CD spectra at pH 7 – 9. For the Cu(II)-Allo1A 3:1 metal-to-ligand molar ratio system three *d-d* transition bands are observed (Table 2, Figure S6). The $\log K^*$ values of the Cu(II)-Allo1A (-46.34) and Cu(II)-Allo1K (-49.72) [28] systems suggest higher stability of the $Cu_3H_{.7}L$ complex of the Allo1A peptide in comparison to that of the $Cu_3H_{.7}(LH)$ complex (Lys residue is protonated) of the Allo1K. For the Allo1K peptide, the $Cu_3H_{.5}L$ complex dominates in the 6.5 – 9.5 pH range [28]. The $pK(\text{amide})$ values in the copper(II) complexes for both peptides are different (Table 1) [28]. These values are lower for the Allo1A complexes. Further deprotonation reactions take place (Figure 5a) and these are accompanied with the spectral changes (Table 2). At pH above 10.5 the $Cu_3H_{.9}L$ and $Cu_3H_{.10}L$ complexes are present in solution with $4N \{NH_2, 3N^-\}$ $4N \{N_{Im}, 3N^-\}$ coordination modes.

For the tri- (Allo1A and Allo9A peptides) and tetranuclear complexes of the Allo1A peptide, significant EPR line broadening is observed. Significant EPR line broadening suggests some spin-spin interactions between the coordinated Cu(II) ions, indicating that paramagnetic copper(II) ions are close to each other. The broadening of the EPR line may be due to dipolar as well as exchange interaction between copper(II) ions [63]. The exchange interaction produces the collapse of the four hyperfine lines, according to the Anderson exchange model [64]. Because the observed line width does not change by increasing or decreasing the concentration (data not shown), this indicates an association of the complexes into larger aggregates, leading to the concentration-independent line broadening by dipolar interactions [65].

For the 3:1 metal-to-ligand molar ratio of the Cu(II)-Allo9A system, the $Cu_3H_{.6}L$ and $Cu_3H_{.10}L$ complexes dominate (Figure 5b) in the 6.5 – 8 and above 9.5 pH range, respectively. The stoichiometry of the $Cu_3H_{.6}L$ complex and the spectroscopic parameters of UV-vis, CD and EPR spectra (Table 3) may suggest $3N \{NH_2, 2N^-, CO\}$ $3N \{N_{Im}, 2N^-\}$ $3N \{N_{Im}, 2N^-\}$ binding modes around three metal ions. The deprotonation and coordination of the amide nitrogen atoms to copper(II) ions for the Allo9A peptide occur at lower pH (Table 1) in comparison to those of the Allo6A and Allo12A peptides [27]. Therefore, it is clear that the $Cu_3H_{.6}L$ complex of the Allo9A dominates at pH 7.2 – 7.3, while this complex of the Allo6A and Allo12A dominate at pH 8.0 – 8.5 [27]. The $\log K^*$ values of the Cu(II)-Allo9A (-40.41), Cu(II)-Allo12A (-42.03) and Cu(II)-Allo6A (-43.25) systems suggest higher stability of the $Cu_3H_{.6}L$ complex of the Allo9A (H^1, H^6, H^{12} are coordinated) in comparison to those of

Allo12A (H^1, H^6, H^9) and Allo6A (H^1, H^9, H^{12}). At pH above 9.5 the Cu_3H_9L and $Cu_3H_{10}L$ complexes dominate (Figure 5b). The stoichiometry of the Cu_3H_9L complex and the transition energy of the $d-d$ at 536 nm suggest the $4N \{NH_2, 3N^-\} 4N \{N_{Im}, 3N^-\} 4N \{N_{Im}, 3N^-\}$ coordination modes (Table 3, Figure S7a). The $\log K^*$ values of the Cu(II)-Allo9A (-66.23) and Cu(II)-Allo12A (-70.01) systems suggest higher stability of the Cu_3H_9L complex of the Allo9A in comparison to that of the Allo12A. The Allo9A peptide forms the Cu_3H_9L complex with the formation, likely, the (6,5,5)(7,5,5)(6,5,5) chelate rings, while the Allo12A forms the this species with the chelate rings (6,5,5)(7,5,5)(7,5,5). Coordination of copper(II) ions to the imidazole nitrogen atoms promotes the deprotonation and metal binding of amide groups towards the C-termini in the form of (7,5,5)-membered chelates [66,67]. The thermodynamic stability of the peptide complexes having this coordination mode is smaller than those formed in the form of (6,5,5)-membered chelates [67-71].

The ESI-MS spectra obtained for the Cu(II)-Allo1A and Cu(II)-Allo9A 3:1 metal-to-ligand molar ratio system recorded in the positive mode show dominant molecular ion $[Cu_3H_4L]^{2+}$ (692.7 Da). For the Cu(II)-Allo1A 4:1 metal-to-ligand molar ratio tetranuclear complexes in MS experiment were not observed.

3.6. Tetranuclear complexes of the Allo1A peptide

Table 1 and the corresponding speciation curve (Figure 6) reveal that tetranuclear species are also formed in the copper(II)-Allo1A system, similar to that of the Cu(II)-Allo1K system [28]. As it is seen on Figure 6, tetranuclear species are formed at pH above 6, similar to that of Allo1K system [28]. However, for the Cu(II)-Allo1A system the Cu_4H_9L species exists in solution in wide 6 – 10 pH range, while for the Cu(II)-Allo1K the $Cu_4H_8(LH)$ (Lys residue is protonated). For the Cu_4H_9L species of the Cu(II)-Allo1A system the $d-d$ transition energy at 611 nm and CD spectra (Table 2, Figure S8) suggest the $4N \{NH_2, 3N^-\}$, $3 \times 3N \{N_{Im}, 2N^-\}$ binding modes around four metal ions. The $\log K^*$ values of the Cu(II)-Allo1A (-61.98) and Cu(II)-Allo1K (-64.89) systems suggest higher stability of the Cu_4H_9L complex of the Allo1A peptide in comparison to that of the Allo1K [28]. With increasing pH (8.5 – 11) three deprotonation reactions take place and these are accompanied with the spectral changes characteristic for the $4N \{NH_2, 3N^-\}$, $2 \times 4N \{N_{Im}, 3N^-\}$, $3N \{N_{Im}, 2N^-, OH^-\}$ binding sites for the $Cu_4H_{12}L$ species (Figures S7b, S8 and S9).

4. Biological Activity

4.1. Phenoloxidase activity assay

The innate immune system in insects is composed of a large variety of specific and nonspecific responses that are activated in response to the presence of foreign agents. One important element in such responses is the enzyme phenoloxidase (PO) [72]. The research has documented PO as an important tool used against several pathogens (bacterial gram + and -, fungal and viral) [73]. Phenoloxidase produces indole groups, which are subsequently polymerized to melanin. Melanin fills many roles in invertebrates besides pigmentation. Several studies have shown that mechanical injury or the presence of macropathogens results in melanin deposition around the damaged tissue or foreign object. This process is commonly known as melanization [73,74]. Phenoloxidase is a member of the tyrosinase group whose main function is to oxidize phenols. All tyrosinases have in common a binuclear type 3 copper center within their active site. This copper center is surrounded by three histidine residues [75]. Phenoloxidases are expressed as inactive zymogens (proPO) in all insects and are converted to active PO when required [72]. Soderhall et al. have reported that the proPO system of invertebrate hemocyte lysates are activated specifically by either β -1,3-glucan from fungal cell wall or lipopolysaccharides and peptidoglycans from bacterial cells [76]. It has found that such factors as temperature and calcium concentration also effect proPO system activation [77,78]. Now we would like to know if the peptides studied (alloferon and its analogues) and their copper(II) complexes may activate phenoloxidase in the *Tenebrio molitor*.

Figure 7a shows the effect of tested compounds on humoral response in *T.molitor*. Injections of alloferon did not have a statistically significant effect on the phenoloxidase activity when compared to control beetles. However, phenoloxidase activity was significantly lower in beetles receiving analogue Allo1A or Allo9A. On the other hand, the analogue Allo1K injection slightly increased level of phenyloxidase activity in *T. molitor*. Generally, copper(II) complexes of all studied analogues significantly increased phenoloxidase activity in *T. molitor*, but the highest increase in enzyme activity was observed after injection of Cu(II)–Allo9A. As it is seen on Figure 1b, at pH 7.4 the CuL complex dominates in solution with the 4N {NH₂,N_{Im}-H¹, N_{Im}-H⁶, N_{Im}-H¹²} coordination mode. In this complex three His residues of the Allo9A are coordinated to copper(II) ions. It is the first report that analogues of alloferon have immunomodulation activity in insects.

4.2. *In vivo* haemocyte bioassay

The representative images in Figures 7b and 8 show the effect of the studied peptides and their copper(II) complexes on the *T. molitor* haemocytes. The *in vivo* bioassay on the *T. molitor* haemocytes showed that Allo9A and its Cu(II) complex were potent because one hour after injection of the 10 nM solution of Allo9A or its copper(II) complex haemocytes' viability and morphology was drastically changed. The most active was Cu(II)-Allo9A (Figure 7b), it retained more than 100% of activity of alloferon, whereas analogue Allo9A showed 12% of pro-apoptotic activity of alloferon (Table 4). Control haemocytes formed extensive filopodia, in which the F-actin microfilaments were detected supcortically after the cells had been allowed to adhere to the cover slips. In all studied individuals, injection of native peptide, Allo9A or Cu(II)-Allo9A caused failure of F-actin organization in haemocytes. They lost their regular F-actin staining pattern as a result of depolymerization of F-actin microfilaments. Moreover, 1-hour exposure of the *Tenebrio molitor* haemocytes to the studied peptides induced in these cells malformations that are typical for an apoptotic morphology, such as cell shrinkage, rounding up and fragmentation of nuclei (Figure 8). Analogue Allo1A did not change haemocytes' viability and morphology compared with control haemocytes. However, its copper(II) complex strongly stimulated the filopodia formation as shown in Figures 8D and 8E. Analogue Allo1K and its Cu(II) complex show weak pro-apoptotic effect (21% and 18% of alloferon activity, respectively) on haemocytes of *T. molitor*. However, these compounds caused the F-actin cytoskeleton changes, but the effect of Cu(II)-Allo1K was stronger than Allo1K. In the *T. molitor* haemocytes, F-actin was found aggregating into distinctive patches after injection of Allo1K or its copper(II) complex (Figures 8J and 8K). The F-actin cytoskeleton changes may be responsible for the observed inhibition of adhesion of haemocytes and for the inhibition of filopodia formation. Moreover, the percentage of apoptotic cells increased after injection of Cu(II)-Allo9A analogue (55% of haemocytes displayed caspase activity) when compared to Allo9A peptide (20% of activated haemocytes). It is interesting that similar data we observed for Cu(II)-Allo12A [27]. Additionally, as shown in Figure 7b injection of Cu(II)-Allo1A and Cu(II)-Allo1K resulted in a decreased the rate of apoptotic haemocytes. These peptides displayed the lowest hemocytotoxic activity among tested copper(II) complex of alloferon analogues. These results indicated that the N-terminal and H⁶ histidine residues are more important for the pro-apoptotic properties in insects than histidine at positions 9 and 12 of the peptide chain of alloferon 1. It should be mentioned that three histidine residues of the Allo9A {NH₂,N_{1m}-H¹,

N_{Im-H^6} , $N_{Im-H^{12}}$ or Allo12A $\{NH_2, N_{Im-H^1}$, N_{Im-H^6} , $N_{Im-H^9}\}$ are coordinated to the copper(II) ions.

4.3. *In vitro semi-isolated heart bioassay*

The knowledge about copper metabolism in the cardiovascular system is very limited, but many clinical and experimental studies have produced data regarding the change in copper concentrations in the blood under cardiovascular disease conditions, including coronary artery disease [79], myocardial infarction [80], diabetic cardiomyopathy [81], cardiac hypertrophy [82], atherosclerosis [83], and other cardiovascular diseases [84]. However, it is difficult to extrapolate the relationship between the increase or decrease in serum copper concentrations and the progression of cardiovascular diseases [85]. The effects of the peptides on the heart contractile activity of *Tenebrio molitor* were established [86,87]. The biological investigation of alloferon and its selected analogues on the myotropic activity in insects were performed [9]. Alloferon induced the cardiostimulatory effect on the heart of *Zophobas atratus*, however, the heart of *Tenebrio molitor* was insensitive to alloferon. Now, we tested the analogues of alloferon 1 and their copper(II) complexes on the heart of *Tenebrio molitor*.

The bioassay *in vitro* on the heart of *T. molitor* showed that application of alloferon analogues or their copper(II) complexes didn't change heartbeat frequency and power of contractions. All tested were inactive on the myocardium of this beetle at the 10^{-7} and 10^{-5} M concentration (Figure 9). However, copper(II) complexes of Allo1A, Allo9A and Allo1K are slightly more active than the free ligands itself at the 10^{-5} M concentration.

5. Conclusion

Here we report the characterization of the copper(II) complexes with the alloferon 1 mutants Allo1A and Allo9A by means of potentiometry, CD, EPR and UV-vis spectroscopic techniques, and ESI-MS spectrometry. The Allo1A peptide forms the mononuclear copper(II) complexes similar to those of the Allo1K [28]. The stability constants of mononuclear copper(II) complexes for both ligands are similar to each other. The CuHL and CuL complexes (CuH₂L and CuHL of Allo1K) dominate in wide 4 – 8 pH range with 3N $\{NH_2, CO, 2N_{Im}\}$ binding sites. At physiological pH 7.4 the CuH₁L complex is present in solution with 3N $\{NH_2, N^-, CO, N_{Im}\}$ coordination mode. The stability of polynuclear complexes of the Allo1A peptide is higher in comparison to those of the Allo1K. Different distribution diagrams obtained for the 2:1, 3:1 and 4:1 metal-to-ligand molar ratios for both peptides (Allo1A and Allo1K) result likely from the presence of the coordination isomers and

the difference in their ratio. It should be mentioned that the mononuclear complexes of the Allo1A and Allo1K are similar to those of alloferon 2 [46]. The presence of the His residue in first position of the Allo9A, Allo6A, Allo12A and alloferon 1 changes their coordination modes to copper(II) ions in comparison to those containing Lys or Ala amino acid residues. The Allo9A, Allo6A and Allo12A peptides form the CuL complex in wide 4.5 – 8.5 pH range with the 4N {NH₂,N_{Im}-H¹,2N_{Im}} binding mode. The stability of this complex follows the order Allo9A (H¹,H⁶,H¹²; 12.57) ~ Allo6A (H¹,H⁹,H¹²; 12.33) > Allo12A (H¹,H⁶,H⁹; 10.90). It should be mentioned that the stabilization of the copper(II) complexes may result not only from the chelate size but also from structural organization of the peptide in the complex [88]. For the metal-to-ligand 2:1 and 3:1 molar ratios the di- and trinuclear complexes dominate at pH above 5.5 and 6.5, respectively. For these peptides different dominant complexes in solution are observed because of the presence of different coordination isomers.

The peptides tested did not cause changes in the frequency (chronotropic response) or amplitude (inotropic response) of heart contractions although they cause the hemocytotoxic effect. Lack of heart response to alloferon and its analogues suggests that it does not affect the mechanical and bioelectrical function of myocardium and does not have cytotoxic influence on cells in this tissue.

The Allo1A and Allo1K and their copper(II) complexes displayed the lowest haemocytotoxic activity among tested copper(II) complexes of alloferon analogues. The most active was the Cu(II)-Allo9A complex formed at pH 7.4 with 4N {NH₂,N_{Im}-H¹,N_{Im}-H⁶,N_{Im}-H¹²} binding site. Similar data were observed for the Cu(II)-Allo12A system at pH 7.4 with similar binding site but different coordination isomer. It may suggest that the copper(II) complex with the coordination of histidine residues H¹, H⁶ and H⁹ or H¹² of the peptide chain has higher proapoptotic properties in insects than those not containing His residue at first position. The coordination to copper(II) ions of the N-terminal amine group and imidazole nitrogen atoms of three His residues creates the macrochelates, the structure of which may be responsible for the biological activity.

Results from all three bioassays indicate that the action of alloferon analogues is tissue-specific and relies on modulation of immune system function in *T. molitor*.

6. Abbreviations

HBTU – 2-(1H-benzotriazole-1-yl)-1,1,3,3-tetramethyluronium hexafluorophosphate

HOBt – 1-hydroxybenzotriazole

Fmoc – 9-fluorenylmethoxycarbonyl

DMF – *N,N*-dimethylformamide

TFA – trifluoroacetic acid

EDT – 1,2-ethanedithiol

ESI-MS – Electrospray Ionization Mass Spectrometry

FT-ICR – Fourier Transform Ion Cyclotron Resonance

CD – Circular Dichroism

MS – Mass Spectrometry

MOPS – 3-(*N*-morpholino)propanesulfonic acid

NK- Natural Killer

UVB – Ultraviolet B (280-315 nm)

UV-vis – UV-visible

M_{calc} – molecular mass calculated

DL- DOPA – *DL*-3,4-dihydroxyphenylalanine

PO – phenoloxidase

SR-VAD-FMK – sulforhodamine-Val-Ala-Asp-fluoromethylketone

DAPI - 4',6-diamidino-2-phenylindole

MFI - Mean Fluorescence Intensity

SD – Standard Deviation

Acknowledgments: Financial support from the Polish Ministry of Science and Higher Education Grant NN 204085638 is gratefully acknowledged. The authors thank to Arkadiusz Urbański and Szymon Chowański for their technical assistance in the biological experiments.

References

- [1] S. Chernysh, S.I. Kim, G. Bekker, V.A. Pleskach, N.A. Filatova, V.B. Anikin, V.G. Platonov, P.Bulet, Proc. Natl. Acad. Sci. U.S.A. 99 (2002) 12628 – 12632.
- [2] N. Lee, S. Bae, H. Kim, J.M. Kong, H.R. Kim, B.J. Cho, S.J. Kim, S.H. Seok, Y.I. Hwang, S. Kim, J.S. Kang, W.J. Lee, Antivir. Ther. 16 (2011) 17 – 26.
- [3] S. Chernysh, I. Kozuharova, I. Artsibasheva, Int.Immunopharm. 12 (2012) 312 – 314.
- [4] Y. Kim, S.K. Lee, S. Bae, H. Kim, Y. Park, N.K. Chu, S.G. Kim, H-R. Kim, Y-il Hwang, J.S. Kang, W.J. Lee, Immun. Lett. 149 (2013) 110 – 118.
- [5] S. Bae, K.Oh, H. Kim, Y. Kim, H-R. Kim, Y-i Hwang, D-S Lee, J.S. Kang, W.J. Lee, Immunobiol. 218 (2013) 1026 – 1033.
- [6] S. Chernysh, I. Kozuharova, Int. Immunopharm. 17 (2013) 1090 – 1093.
- [7] J.J. Docherty, J.J. Pollock, Antimicrob. Agents Chemother. 31 (1987) 1562 – 1566.
- [8] M. Kuczer, A. Midak-Siwierska, R. Zahorska, M. Łuczak, D. Konopińska, J. Pep. Sci. 17 (2011) 715 – 719.
- [9] M. Kuczer, E. Czarniewska, G. Rosiński, Regul. Peptides 183 (2013) 17 – 22.
- [10] K. Kochman, A. Gajewska, H. Kochman, H. Kozłowski, E. Masiukiewicz, B. Rzeszotarska, J. Inorg. Biochem. 65 (1997) 277 – 279.
- [11] A. Herman, H. Kozłowski, M. Czauderna, K. Kochman, K. Kulon, A. Gajewska, J. Physiol. Pharm. 63 (2012) 69 – 75.
- [12] L. Mazur, B. Modzelewska-Banachiewicz, R. Paprocka, M. Zimecki, U.E. Wawrzyniak, J. Kutnowska, G. Ziółkowska, J. Inorg. Biochem. 114 (2012) 55 – 64.
- [13] A.I. Matesanz, P. Souza, J. Inorg. Biochem. 101 (2007) 245 – 253.
- [14] A. Garoufis, S.K. Hadjidakou, N. Hadjiliadis, Coord. Chem. Rev. 253 (2009) 1384 – 1397.
- [15] K. Alomar, A. Landreau, M. Kempf, M.A. Khan, M. Allain, G. Bouet, J. Inorg. Biochem. 104 (2010) 397 – 404.
- [16] J. Lessa, K.O. Ferraz, J. Guerra, L. Miranda, C.D. Romeiro, E. Souza-Fagundes, P. Barbeira, H. Beraldo, BioMetals, 25 (2012) 587 – 598.
- [17] K. Alomar, A. Landreau, M. Allain, G. Bouet, G. Larcher, J. Inorg. Biochem. 126 (2013) 76 – 83.
- [18] M.J. McKeage, S.J. Berners-Price, P. Galettis, R.J. Bowen, W. Brouwer, L. Ding, L. Zhuang, B.C. Baguley, Cancer Chemoth. Pharm. 46 (2000) 343 – 350.
- [19] E. Czarniewska, L. Mrówczyńska, M. Kuczer, G. Rosiński, J. Ex. Biol. 215 (2012) 4308 – 4313.

- [20] G-J. Chen, X. Ciao, P-Q. Qia, G.-J. Xu, J-Y. Xu, J-L Tian, W. Gu, X. Liu, S-P. Yan, J. *Inorg. Biochem.* 105 (2011) 119 – 126.
- [21] Z-Y. Ma, X. Qiao, Ch-Z. Xie, J. Shao, J-Y. Xu, Z-Y. Qiang, J-S. Lou, J. *Inorg. Biochem.* 117 (2012) 1 – 9.
- [22] J. Zuo, C. Bi, Y. Fan, D. Buac, Ch. Nardon, K.G. Daniel, Q.P.Dou, J. *Inorg. Biochem.* 118 (2013) 83 – 93.
- [23] S.E.F. Gonzalez, E.A. Anguiano, A.M. Herrera, D.E. Calzada, C.O. Pichardo, *Toxicology* 314 (2013) 155 – 165.
- [24] S.S. Habbeebu, J. Liu, C.D. Klaassen, *Toxicol. Appl. Pharm.* 149 (1998) 203 – 209.
- [25] H. Ras, B.P. Braekman, G.R.J. Criel, V. Rzeznik, J.R. Vanfleteren, *J. Ex. Zool.* 286 (2000) 1 – 12.
- [26] S.H. Lee, D.K. Kim, Y.R. Seo, K.M. Woo, C.S. Kim, M.H. Cho, *Exp. Mol. Med.* 30 (1998) 171 – 176.
- [27] M. Kuczer, M. Błaszak, E. Czarniewska, G. Rosiński, T. Kowalik-Jankowska, *Inorg. Chem.* 52 (2013) 5951 – 5961.
- [28] M. Kuczer, M. Pietruszka, T. Kowalik-Jankowska, *J. Inorg. Biochem.* 111 (2012) 40 – 49.
- [29] H. Irving, M.G. Miles, L.D. Pettit, *Anal. Chim. Acta* 38 (1967) 475 – 488.
- [30] G. Gans, A. Sabatini, A. Vacca, *J. Chem. Soc. Dalton Trans.* (1985) 1195 – 1199.
- [31] P. Gans, A. Sabatini, A. Vacca, *Talanta* 43 (1996) 1739 – 1753.
- [32] G. Gran, *Acta Chem. Scand.* 4 (1950) 559 – 577.
- [33] G. Rosiński, A. Wrzeszcz, L. Obuchowicz, *Insect. Biochem.* 9 (1979) 485 – 488.
- [34] D. Ludwig, C. Fiore, *Ann. Entomol. Soc.Am.* 53 (1960) 595 – 600.
- [35] D. Ludwig, C. Fiore, R. Jones, *Ann. Entomol. Soc.Am.* 55 (1962) 439 - 442.
- [36] G. Rosiński, *Zool. Series 22*, Adam Mickiewicz University Press; Poznań, 1995 1 - 148.
- [37] N.E. Good, G.D. Winget, W. Winter, I.N. Connolly, S. Izawa, R.M.M. Singh, *Biochemistry* 5 (1966) 467 – 477.
- [38] R.P. Sorrentino, C.N. Small, S. Govind, *Biotechniques* 32 (2002) 815 – 822.
- [39] G. Rosiński, G. Gade, *J. Insect Physiol.* 34 (1988) 1035 - 1042.
- [40] R.W. Hay, M.M. Hassan, C. You-Quan, *J. Inorg. Biochem.* 52 (1993) 17 – 25.
- [41] N.I. Jakab, B. Gyurcsik, T. Kortvelyesi, I. Vosekalna, J. Jensen, E. Arsen, *J. Inorg. Biochem.* 101 (2007) 1376 – 1385.
- [42] A. Travaglia, D. La Mendola, A. Magri, V.G. Nicoletti, A. Pietropaolo, E. Rizzarelli, *Chem. Eur. J.* 18 (2012) 15618 – 15631.

- [43] A. Grenacs, A. A. Kaluha, C. Kallay, V. Jozsai, D. Sanna, I. Sovago, J. Inorg. Biochem. 128 (2013) 17 – 25.
- [44] W. Bal, H. Kozłowski, G. Kupryszewski, Z. Maćkiewicz, L.D. Pettit, R. Robbins, J. Inorg. Biochem. 52 (1993) 79 – 87.
- [45] J.F. Galey, B. Decock-Le Reverend, A. Lebdiri, L.D. Pettit, S.I. Pyburn, H. Kozłowski, J. Chem. Soc. Dalton Trans. (1991) 2281 – 2287.
- [46] T. Kowalik-Jankowska, Ł. Biega, M. Kuczer, D. Konopińska, J. Inorg. Biochem. 103 (2009) 135 – 142.
- [47] E. Prenesti, P.G. Daniele, M. Prencipe, G. Ostacoli, Polyhedron 18 (1999) 3233 – 3241.
- [48] K. Varnagy, J. Szabo, I. Sovago, G. Malandrinos, N. Hadjiliadis, D. Sanna, G. Micera, J. Chem. Soc. Dalton Trans. (2000) 467 – 472.
- [49] I. Sovago, C. Kallay, K. Varnagy, Coord. Chem. Rev. 256 (2012) 2225 – 2233.
- [50] M. Moini, Rapid Commun. Mass Spectrom. 24 (2010) 2730 – 2734.
- [51] M. Keith-Roach, Anal. Chim. Acta 678 (2010) 140 – 148.
- [52] R. Sekar, S.K. Kailasa, H.N. Abdelhamid, Y-Ch. Chen, H-F. Wu, Int. J. Mass Spectrom. 338 (2013) 23 – 29.
- [53] V.G. Shtyrlin, Y.I. Zyavkina, E.M. Gilyazetdinov, M.S. Bukharov, A.A. Krutikov, R.R. Garipov, A.S. Mukhtarov, A.V. Zakharov, Dalton Trans. 41 (2012) 1216 – 1228.
- [54] T. Kowalik-Jankowska, M. Ruta-Dolejsz, K. Wiśniewska, L. Łankiewicz, J. Inorg. Biochem. 95 (2003) 270 – 282.
- [55] T. Kowalik-Jankowska, M. Ruta-Dolejsz, K. Wiśniewska, L. Łankiewicz, J. Inorg. Biochem. 86 (2001) 535 – 545.
- [56] Z. Paksi, A. Jancso, F. Pacello, N. Nagy, A. Battistoni, T. Gajda, J. Inorg. Biochem. 102 (2008) 1700 – 1710.
- [57] T. Kowalik-Jankowska, M. Jasionowski, L. Łankiewicz, J. Inorg. Biochem. 76 (1999) 63 – 70.
- [58] K. Osz, K. Varnagy, H. Suli-Vargha, D. Sanna, G. Micera, I. Sovago, Dalton Trans. (2003) 2009 – 2016.
- [59] T. Gajda, B. Henry, A. Aubry, J.-J. Delpuech, Inorg. Chem. 35 (1996) 586 – 593.
- [60] T.G. Fawcett, E.E. Bernarducci, K. Krogh-Jespersen, H.J. Schugar, J. Am. Chem. Soc. 102 (1980) 2598 – 2604.
- [61] E. Prenesti, P.G. Daniele, S. Berto, S. Toso, Polyhedron 25 (2006) 2815 – 2823.
- [62] S. Timari, C. Kallay, K. Osz, I. Sovago, K. Varnagy, Dalton Trans. (2009) 1962 – 1971.

- [63] C.A. Stern, A.M. Gennaro, P.R. Levstein, R. Calvo, *J. Phys. Condens. Matter* 1 (1989) 637 – 642.
- [64] P.W. Anderson, *Phys. Soc. Jpn.* 9 (1954) 316 – 339.
- [65] T. Glaser, M. Heidemeier, F.E. Hahn, T. Lugger, *Z. Naturforsch.* 58b (2003) 505 – 510.
- [66] C.S. Burns, E. Aronoff-Spencer, C.M. Dunham, P. Lario, N.I. Avdievich, W.E. Antholine, M.M. Olmstead, A. Vrieling, G.J. Gerfen, J. Peisach, W.G. Scott, G.L. Millhauser, *Biochemistry* 41 (2002) 3991 – 4001.
- [67] G. Di Natale, K. Osz, C. Kallay, G. Pappalardo, D. Sanna, G. Impellizzeri, I. Sovago, E. Rizzarelli, *Chem.-Eur. J.* 19 (2013) 3751 – 3761.
- [68] G. Di Natale, G. Grasso, G. Impellizzeri, D. La Mendola, G. Micera, N. Mihala, Z. Nagy, K. Osz, G. Pappalardo, V. Rigo, E. Rizzarelli, D. Sanna, I. Sovago, *Inorg. Chem.* 44 (2005) 7214 – 7225.
- [69] K. Osz, Z. Nagy, G. Pappalardo, G. Di Natale, D. Sanna, G. Micera, E. Rizzarelli, I. Sovago, *Chem. Eur. J.* 13 (2007) 7129 – 7143.
- [70] G. Di Natale, K. Osz, Z. Nagy, D. Sanna, G. Micera, G. Pappalardo, I. Sovago, E. Rizzarelli, *Inorg. Chem.* 48 (2009) 4239 – 4250.
- [71] C.E. Jones, S.R. Abdelraheim, D.R. Brown, J.H. Viles, *J. Biol. Chem.* 279 (2004) 32018 – 32027.
- [72] I. Gonzalez-Santoyo, A. Cordoba-Aquilar, *Entomol. Exp. Appl.* 142 (2012) 1-16.
- [73] L. Cerenius, K. Soderhall, *Immunol. Rev.* 198 (2004) 116 – 126.
- [74] A.J. Nappi, B.M. Christensen, *Insect Biochem. Molec.* 35 (2005) 443 – 459.
- [75] E. Jaenicke, H. Decker, *Biochem. J.* 371 (2003) 515 – 523.
- [76] K. Soderhall, L. Cerenius and M.W. Johansson, *Ann. N. Y. Acad. Sci.* 712 (1994) 155 – 161.
- [77] B. Dularay, A.M. Lackie, *Insect Biochem.* 15 (1985) 827 – 834.
- [78] H.-H. Sung, H.-J. Chang, Ch.-H. Her, J.-Ch. Chang, Y.-L. Song, *J. Inver. Pathol.* 71 (1998) 26 – 33.
- [79] E.S. Ford, *Am. J. Epidemiol.* 151 (2000) 1182 – 1188.
- [80] A. Reunanen, P. Knekt, R.K. Aaran, *Am. J. Epidemiol.* 136 (1992) 1082 – 1090.
- [81] Y. Song, J. Wang, Y. Li, Y. Du, G.E. Arteel, J.T. Saari, J. Kang, L. Cai, *Am. J. Pathol.* 167 (2005) 17 – 26.
- [82] Y. Jiang, C. Reynolds, C. Xiao, W. Feng, Z. Zhou, W. Rodriguez, S.C. Tyagi, J.W. Eaton, J.T. Saari, Y.J. Kang, *J. Exp. Med.* 204 (2007) 657 – 666.

- [83] G.D. Kinsman, A.N. Howard, D.L. Stone, P.A. Mullins, *Biochem. Soc. Trans.* 18 (1990) 1186 – 1188.
- [84] F.J. Kok, C.M. Van Duijn, A. Hofman, G.B. Van der Voet, F.A. Wolff, C.H. Paays, H.A. Valkenburg, *Am. J. Epidemiol.* 128 (1988) 352 – 359.
- [85] Y.J. Kang, *Pharm. Therap.* 129 (2011) 321 – 331.
- [86] P. Marciniak, S. Grodecki, D. Konopińska, G. Rosiński, *J. Pept. Sci.* 14 (2008) 329 – 334.
- [87] K. Szymanowska-Dziubasik, P. Marciniak, G. Rosiński, D. Konopińska, *J. Pept. Sci.* 14 (2008) 708 – 713.
- [88] T. Kowalik-Jankowska, M. Ruta-Dolejsz, K. Wiśniewska, L. Łankiewicz, J. *Inorg. Biochem.* 92 (2002) 1 – 10.

List of Figures

Figure 1. Species distribution diagram for Cu(II) complexes with a) Allo1A, b) Allo9A. Charges are omitted for clarity. [L] = 0.001 M, M/L molar ratio = 1:1.

Figure 2. Schematic of the CuL complex species: a) Allo9A; b) Allo6A; c) Cu₂L₂ complex of the Allo9A.

Figure 3. Species distribution diagram for Cu(II) complexes with a) Allo1A, b) Allo9A. Charges are omitted for clarity. [L] = 0.001 M, M/L molar ratio = 2:1.

Figure 4. ESI mass spectrum for the Cu(II)-Allo1A and Cu(II)-Allo9A systems at 2:1 molar ratio in water solution at pH about 7. Experimental and simulated spectra for the Cu₂H₂L molecular ion with m/z 661.2 Da.

Figure 5. Species distribution diagram for Cu(II) complexes with a) Allo1A, b) Allo9A. Charges are omitted for clarity. [L] = 0.001 M, M/L molar ratio = 3:1.

Figure 6. Species distribution diagram for Cu(II) complexes with Allo1A. Charges are omitted for clarity. [L] = 0.001 M, M/L molar ratio = 4:1.

Figure 7. (a) Humoral response expressed as phenoloxidase (PO) activity in *T. molitor*. Values are given as mean \pm SE. *Significant differences in PO activity between treated groups were observed ($F=7.095$, $p<0.0001$); (b) The rate of apoptotic haemocytes to total haemocytes after injection of *T. molitor*. * Data not include cells which have been fragmented into apoptotic bodies. **Data from literature [27].

Figure 8. Representative fluorescence microscopic images showing *in vivo* induced apoptotic effects in *T. molitor* haemocytes. A, PS; B, MOPS; C, MOPS + Cu(II); D, Allo1; E, Cu(II)-Allo1; F, Allo1A; G, Cu(II)-Allo1A; H, Allo9A; I, Cu(II)-Allo9A; J, Allo1K; K, Cu(II)-Allo1K). All haemocytes were stained with SR-VAD-FMK reagent for caspase activity detection (red color), DAPI for cell nuclei detection (blue color) and Oregon Green–phalloidin for staining of the F-actin cytoskeleton (green color). Arrows show aggregation of F-actin (G, H, J) and apoptotic bodies (I). Scale bars indicate 10 μ m in all panels.

Figure 9. Percentage change in heartbeat frequency after application physiological solution (PS), MOPS+Cu(II), alloferon, its analogues or their Cu(II)-complex. Values are given as mean \pm SE.

ACCEPTED MANUSCRIPT

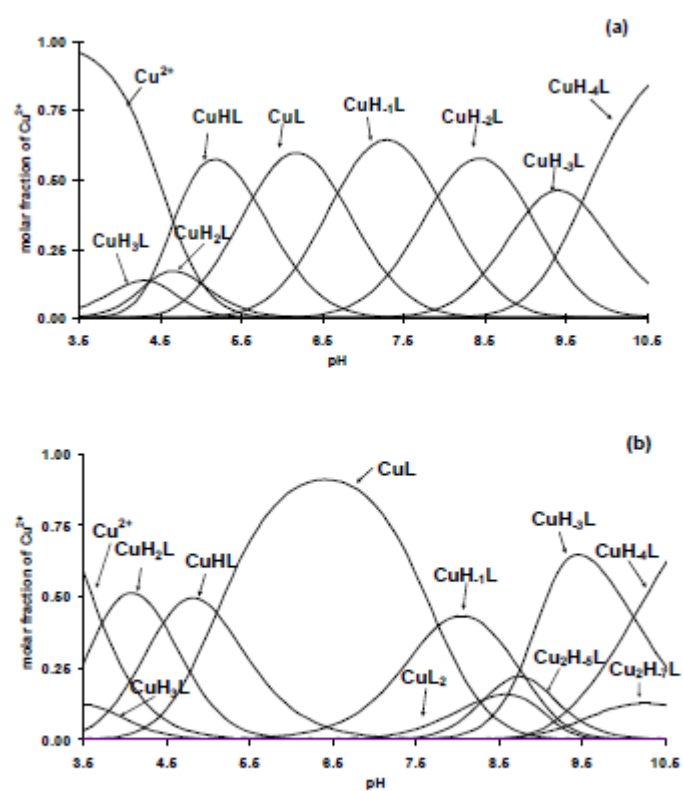


Figure 1

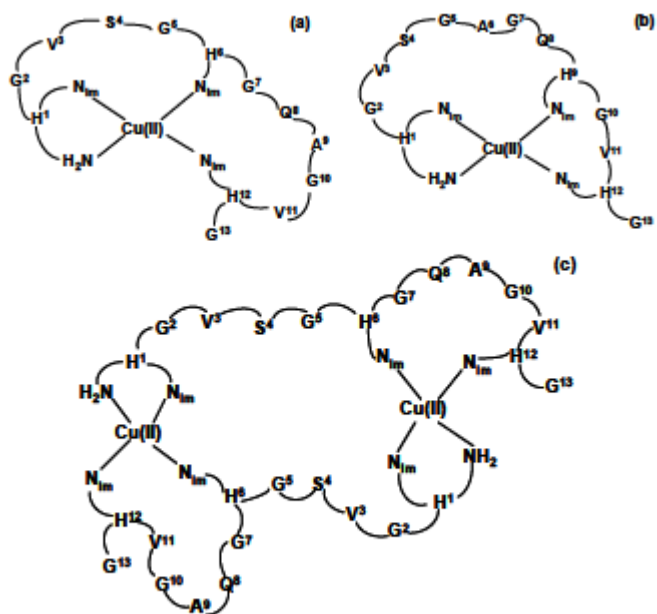


Figure 2

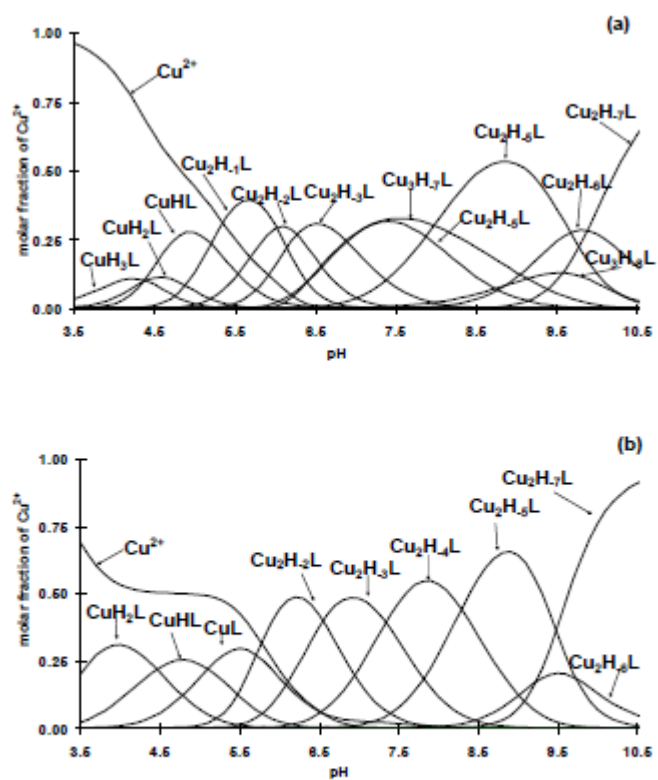


Figure 3

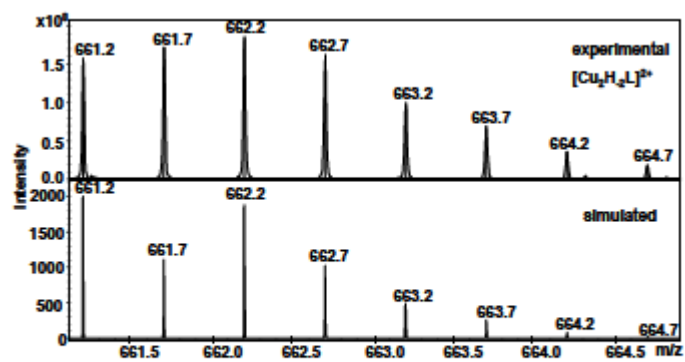


Figure 4

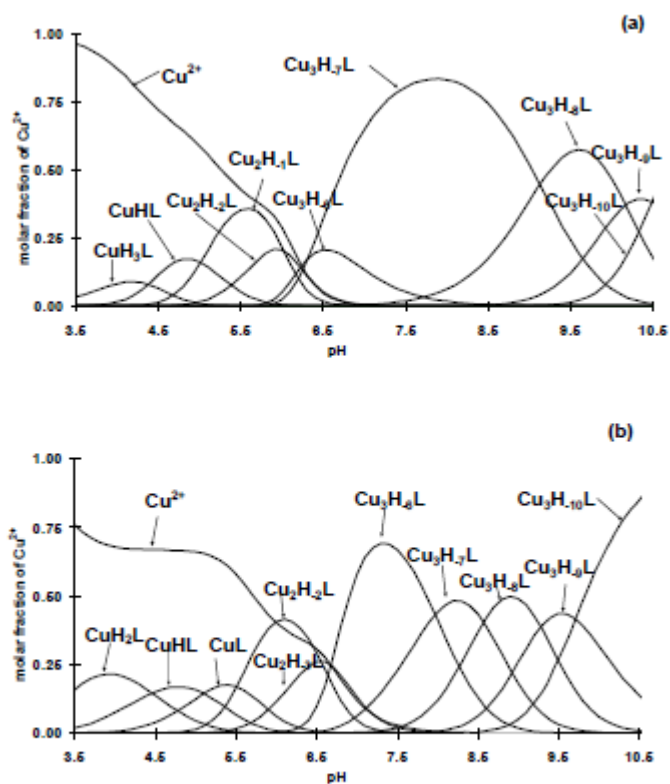


Figure 5

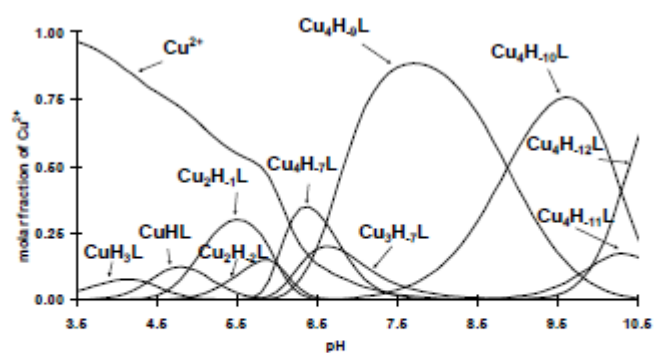


Figure 6

ACCEPTED MANUSCRIPT

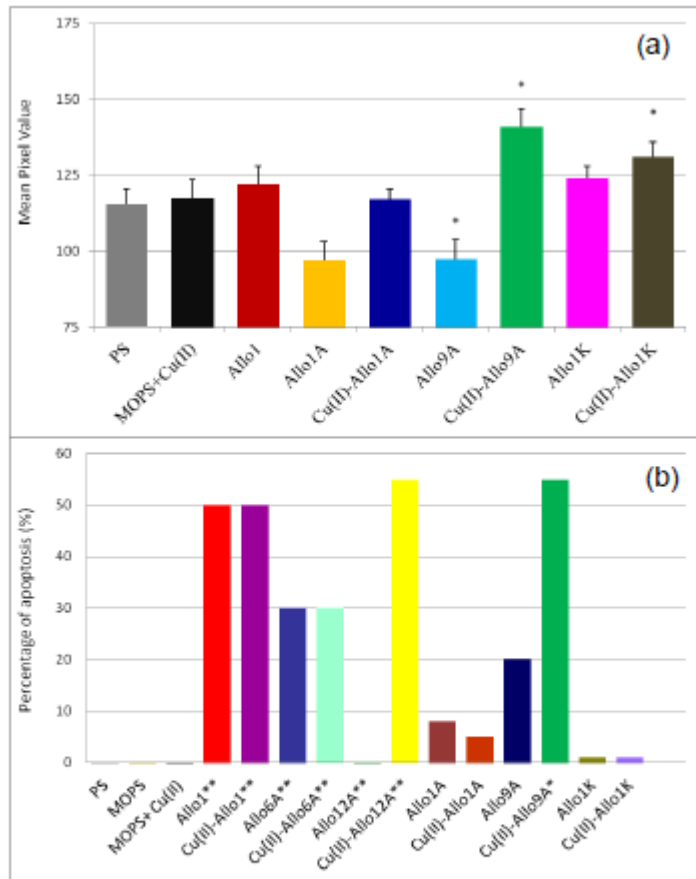


Figure 7

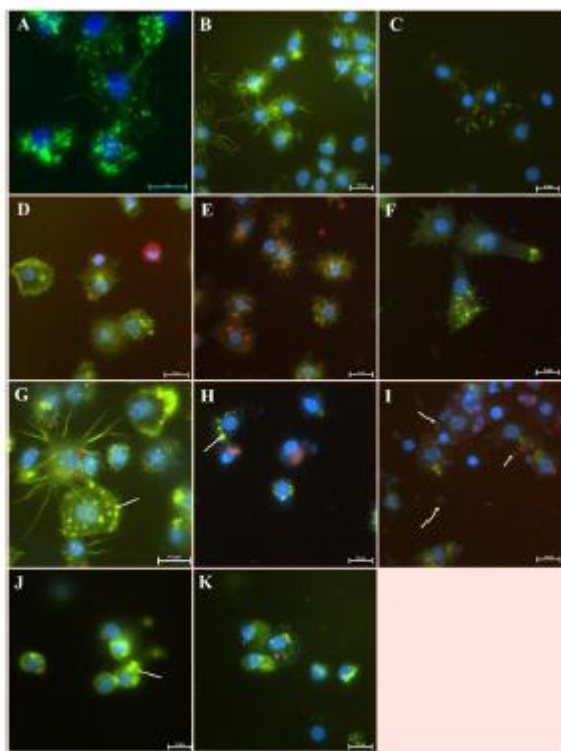


Figure 8

ACCEPTED

SCRIPT

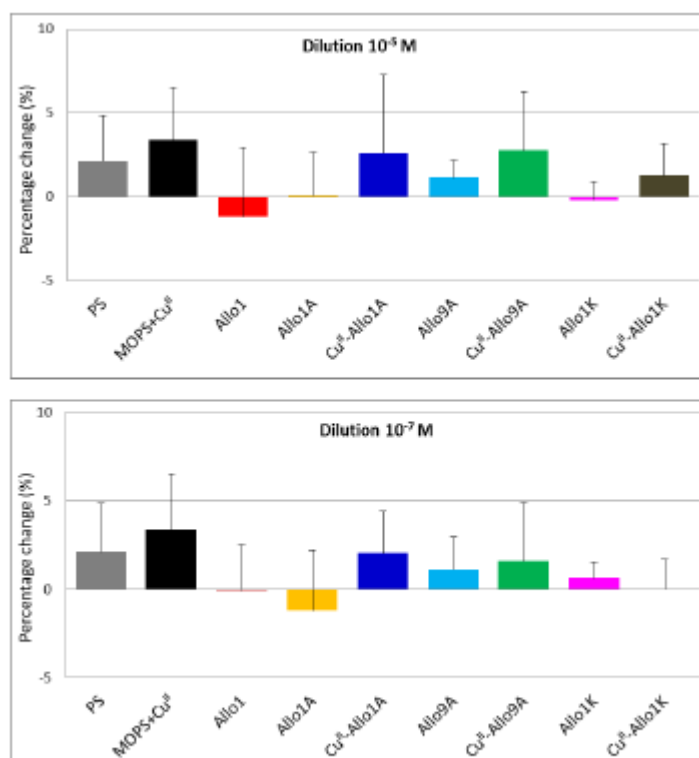
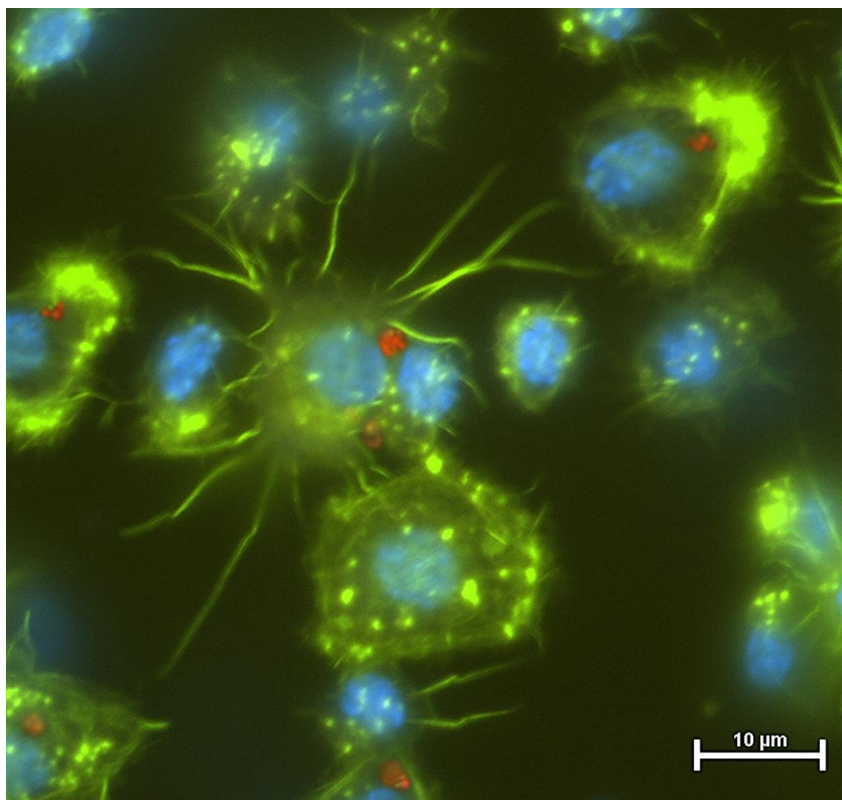


Figure 9



Graphical abstract

Characterization of the Cu(II) complexes with alloferon 1 mutants Allo1A and Allo9A by means of potentiometry, CD, UV-Vis and EPR spectroscopic techniques, and ESI-MS spectrometry is reported. The biological studies are also performed.

ACCEPTED MANUSCRIPT

Table 1. Formation ($\log\beta$) and deprotonation (pK) constants for the Allo1A, Allo9A and their Cu(II) complexes (T=298K, I=0.1M KNO₃).^a

| Species | Allo1A | Allo9A | Species | Allo1A | Allo9A |
|-----------------------|-----------|-----------|-----------------------------------|-----------|-----------|
| HL | 8.03(1) | 7.67(1) | Cu ₂ H ₁ L | 9.25(2) | |
| H ₂ L | 15.05(1) | 14.54(1) | Cu ₂ H ₂ L | 3.23(3) | 4.01(4) |
| H ₃ L | 21.53(1) | 20.79(1) | Cu ₂ H ₃ L | -3.04(3) | -2.54(4) |
| H ₄ L | 27.32(1) | 26.08(1) | Cu ₂ H ₄ L | -9.93(3) | -9.88(4) |
| H ₅ L | 30.48(1) | 29.22(1) | Cu ₂ H ₅ L | -17.80(2) | -18.17(5) |
| pK(NH ₂) | 8.03 | 7.67 | Cu ₂ H ₆ L | -27.47(3) | -27.90(9) |
| pK(His) | 7.02 | 6.87 | Cu ₂ H ₇ L | -37.35(2) | -37.13(5) |
| pK(His) | 6.48 | 6.25 | pK _(-1/-2) | 6.02 | |
| pK(His) | 5.79 | 5.29 | pK _(-2/-3) | 6.27 | 6.55 |
| pK(COO ⁻) | 3.16 | 3.14 | pK _(-3/-4) | 6.89 | 7.34 |
| | | | pK _(-4/-5) | 7.87 | 8.29 |
| CuH ₃ L | 25.57(5) | 25.28(13) | pK _(-5/-6) | 9.67 | 9.73 |
| CuH ₂ L | 21.18(3) | 22.13(2) | pK _(-6/-7) | 9.88 | 9.23 |
| CuHL | 16.82(1) | 17.67(3) | | | |
| CuL | 11.17(1) | 12.57(3) | Cu ₃ H ₆ L | -18.50(6) | -19.62(5) |
| CuH ₁ L | 4.48(1) | 4.80(6) | Cu ₃ H ₇ L | -24.81(2) | -27.59(7) |
| | | | | | |
| CuH ₂ L | -3.44(2) | - | Cu ₃ H ₈ L | -33.94(3) | -36.16(8) |
| CuH ₃ L | -12.48(2) | -12.70(5) | Cu ₃ H ₉ L | -44.11(3) | -45.44(8) |
| CuH ₄ L | -22.17(2) | -22.82(5) | Cu ₃ H ₁₀ L | -54.60(4) | -55.15(7) |
| CuL ₂ | - | 18.12(9) | pK _(-6/-7) | 6.31 | 7.97 |
| pK _(3/2) | 4.39 | 3.15 | pK _(-7/-8) | 9.13 | 8.57 |
| pK _(2/1) | 4.36 | 4.46 | pK _(-8/-9) | 10.17 | 9.28 |
| pK _(1/0) | 5.65 | 5.10 | pK _(-9/-10) | 10.49 | 9.71 |

| | | | | |
|----------------|------|-------|------------------|------------|
| $pK_{(0/-1)}$ | 6.69 | 7.77 | | |
| $pK_{(-1/-2)}$ | 7.92 | 8.75 | Cu_4H_7L | -21.43(7) |
| $pK_{(-2/-3)}$ | 9.04 | 8.75 | Cu_4H_9L | -34.66(2) |
| $pK_{(-3/-4)}$ | 9.69 | 10.12 | $Cu_4H_{10}L$ | -43.54(4) |
| | | | $Cu_4H_{11}L$ | -54.21(11) |
| | | | $Cu_4H_{12}L$ | -64.14(5) |
| | | | $pK_{(-7/-8)}$ | 6.62 |
| | | | $pK_{(-8/-9)}$ | 6.62 |
| | | | $pK_{(-9/-10)}$ | 8.88 |
| | | | $pK_{(-10/-11)}$ | 10.67 |
| | | | $pK_{(-11/-12)}$ | 9.93 |

^a Standard deviations (3σ values) are given in parentheses. Charge are omitted for clarity; $pK(n/m)$ values reflect the pK values of copper(II) complexes.

continuation of Table 1.

Table 2. Spectroscopic data for the mononuclear and polynuclear Cu(II) complexes of Allo1A in the solutions containing 1:1, 2:1, 3:1 and 4:1 metal-to-ligand molar ratios.

| M:L | Species | pH | UV-Vis | | CD | | EPR | |
|---|---|------|-------------------|---|-------------------|---|--|-----------------|
| | | | λ [nm] | ϵ [M ⁻¹ cm ⁻¹] | λ [nm] | $\Delta\epsilon$ [M ⁻¹ cm ⁻¹] | A _{II} [G] | g _{II} |
| 1:1 | CuHL, CuL | 5.3 | | | 662 ^a | -0.135 | 158 | 2.275 |
| | 3N | - | 628 ^a | 81 | 275 ^b | +0.295 | | |
| | {NH ₂ , CO, 2N _{Im} } | 6.0 | | | | | | |
| | CuH₁L | | | | | | | |
| | 3N | | | | 653 ^a | -0.300 | 161 | 2.229 |
| | {NH ₂ , N ⁻ , CO, N _{Im} } | 7.5 | 607 ^a | 93 | 265 ^b | +0.668 | | |
| or 4N {NH ₂ , N ⁻ , 2N _{Im} } | | | | | | | | |
| | CuH₃L, CuH₄L | | | | 600 ^a | -0.187 | 206 | 2.200 |
| | 4N | 9.5 | | | 501 ^a | +0.482 | | |
| | {NH ₂ , 3N ⁻ } | - | 559 ^a | 100 | 319 ^c | -0.096 | | |
| | or {N _{Im} , 3N ⁻ } | 10.5 | | | 275 ^b | +1.065 | | |
| 2:1 | Cu₂H₅L | | | | 607 ^a | -0.380 | broad band Cu(II)- Cu(II) interaction with A _{II} =200, g _{II} =2.195 | |
| | 4N {NH ₂ , 3N ⁻ } | 9.0 | 582 ^a | 92 | 499 ^a | +0.268 | | |
| | 4N {2N _{Im} , 2N ⁻ } | | | | 342 ^d | +0.138 | | |
| | Cu₂H₇L | | | | 586 ^a | -0.526 | broad spectrum Cu(II)-Cu(II) interaction | |
| | 4N {NH ₂ , 3N ⁻ } | 11.0 | 556 ^a | 104 | 492 ^a | +0.621 | | |
| | 4N {2N _{Im} , 2N ⁻ } | | | | 315 ^c | -0.404 | | |

| | | | | | | | |
|------------|---|------|------------------|----|------------------|--------|------------------------------|
| | Cu₃H₇L | | | | 774 ^a | +0.101 | |
| | 4N {NH ₂ , 3N ⁻ } | 7.0 | | | 631 ^a | -0.387 | |
| 3:1 | 4N {2N _{Im} , 2N ⁻ } | - | 613 ^a | 89 | 503 ^a | +0.070 | |
| | 3N {N _{Im} , 2N ⁻ } | 9.0 | | | 337 ^d | +0.499 | broad spectrum |
| | | | | | | | Cu(II)-Cu(II) interaction |
| | Cu₃H₁₀L | | | | 590 ^a | -0.314 | |
| | 4N {NH ₂ , 3N ⁻ } | 11.0 | 562 ^a | 95 | 496 ^a | +0.419 | |
| | 4N {N _{Im} , 3N ⁻ } | | | | 309 ^c | -0.290 | |
| | 4N {N _{Im} , 3N ⁻ } | | | | | | |
| | Cu₄H₉L | | | | 784 ^a | +0.123 | |
| 4:1 | 4N {NH ₂ , 3N ⁻ } | 7.5 | 611 ^a | 90 | 629 ^a | -0.349 | |
| | 3x3N {N _{Im} , 2N ⁻ } | | | | 499 ^a | +0.043 | |
| | | | | | 337 ^d | +0.485 | |
| | Cu₄H₁₀L | | | | 774 ^a | +0.105 | |
| | 4N {NH ₂ , 3N ⁻ } | | | | 635 ^a | -0.259 | broad spectrum |
| | 4N {N _{Im} , 3N ⁻ } | 9.5 | 596 ^a | 89 | 513 ^a | +0.085 | Cu(II)-Cu(II) interaction |
| | 2x3N {N _{Im} , 2N ⁻ } | | | | 335 ^d | +0.330 | |
| | Cu₄H₁₂L | | | | | | |
| | 4N {NH ₂ , 3N ⁻ } | | | | 594 ^a | -0.178 | |
| | 2x4N {N _{Im} , 3N ⁻ } | 11.0 | 558 ^a | 95 | 499 ^a | +0.293 | |
| | 3N {N _{Im} , 2N ⁻ , OH ⁻ } | | | | | | |

^a d-d transition

^b NH₂ → Cu(II) and N_{Im} (π₂) → Cu(II) charge transfer transitions

^c N⁻ (amide) → Cu(II) charge transfer transition

^d N_{Im} (π₁) → Cu(II) charge transfer transition

continuation of Table 2

Table 3. Spectroscopic data for the mononuclear and polynuclear Cu(II) complexes of Allo9A in the solutions containing 1:1, 2:1 and 3:1 metal to ligand molar ratios.

| M:L | Species | pH | UV-Vis | | CD | | EPR | |
|---|--|----------|-------------------|---|---------------------------------------|---|------------------------|-----------------|
| | | | λ [nm] | ϵ [M ⁻¹ cm ⁻¹] | λ [nm] | $\Delta\epsilon$ [M ⁻¹ cm ⁻¹] | A [G] | g |
| CuH₂L | | | | | | | | |
| 1:1 | 2N {NH ₂ , N _{Im} -H ¹ } | 4.0 | 660 ^a | 36 | 318 ^b | -0.066 | 158 | 2.285 |
| CuL | | | | | | | | |
| | 4N {NH ₂ , N _{Im} -H ¹ , N _{Im} -H ⁶ , N _{Im} -H ¹² } | 6.5 | 598 ^a | 79 | 315 ^b | -0.164 | 180 | 2.250 |
| CuH₃L, CuH₄L | | | | | | | | |
| | 4N {NH ₂ , 3N ⁻ } | 9.5 - | 550 ^a | 103 | 508 ^a 284 ^{bb} | +0.302 | 192 | 2.218 |
| | or {N _{Im} , 3N ⁻ } | 10.5 | | | | | | |
| 2:1 | Cu₂H₅L 4N {NH ₂ , 3N ⁻ } | 9.0 | 568 ^a | 91 | 597 ^a 500 ^a | -0.127 +0.275 | 190 | 2.227 |
| | 4N {N _{Im} , 2N ⁻ , N _{Im} } | | | | | | | |
| | Cu₂H₇L 4N {NH ₂ , 3N ⁻ } | 10.5 | 532 ^a | 110 | 594 ^a 494 ^a | -0.375 +0.637 | 200 | 2.204 |
| | 4N {N _{Im} , 3N ⁻ } | | | | 314 ^c | -0.325 | | |

| | | | | | | | |
|------------|--|------|------------------|----|------------------|--------|------------------------------|
| | Cu₃H₆L | | | | 651 ^a | -0.035 | |
| 3:1 | 2N {NH ₂ , N ⁻ , CO} | | | | 535 ^a | +0.080 | |
| | 3N {N _{Im} , 2N ⁻ } | 7.2 | 600 ^a | 71 | 344 ^d | +0.054 | |
| | 3N {N _{Im} , 2N ⁻ } | | | | 302 ^c | -0.063 | broad spectrum |
| | Cu₃H₁₀L | | | | | | Cu(II)-Cu(II) interaction |
| | 4N {NH ₂ , 3N ⁻ } | 9.5 | | | 591 ^a | -0.372 | |
| | 4N {N _{Im} , 3N ⁻ } | - | 536 ^a | 98 | 495 ^a | +0.541 | |
| | 4N {N _{Im} , 3N ⁻ } | 10.5 | | | 313 ^c | -0.291 | |

^a d-d transition

^b NH₂ → Cu(II) and N_{Im}(π₂) → Cu(II) charge transfer transitions

^c N⁻ (amide) → Cu(II) charge transfer transition

^d N_{Im} (π₁) → Cu(II) charge transfer transition

^{bb} broad band

continuation of Table 3

Table 4. Cytotoxicity of alloferon analogues.

| Sample | Number of | MFI±SD | Effect on the caspases |
|---------------|------------------------------|--------------|---------------------------------------|
| | fluorescent cells counted | | activity relative to alloferon (%) |
| PS | 50 | 3.80±0.86 | 0 |
| MOPS | 50 | 3.91±0.86 | 0 |
| MOPS+Cu(II) | 50 | 3.66±1.42 | 0 |
| Allo1 | 50 | 16.87 ± 3.15 | 100 |
| Cu(II)-Allo1 | 50 | 26.31±4.71 | 172 |
| Allo1A | 50 | 4.43 ± 1.6 | 5 |
| Cu(II)-Allo1A | 50 | 5.62±1.9 | 13 |
| Allo9A | 50 | 5.39±2.4 | 12 |
| Cu(II)-Allo9A | * | * | >100* |
| Allo1K | 50 | 6.64±2.17 | 21 |
| Cu(II)-Allo1K | 50 | 6.38±2.73 | 19 |

MFI - mean fluorescence intensity, SD-standard deviation

na – not activity, *the calculation of MFI was impossible, because many apoptotic bodies were observed. Effect on the caspases activity relative to alloferon (%)=[(MFI analogue - MFI PS)/MFI alloferonu – MFI PS] x 100%

Highlights

- >The stoichiometry and stability of Cu(II)-Allo1A and Cu(II)-Allo9A are determined.
- > Structure of the complexes formed is given.
- >The inductions of phenoloxidase activity and apoptosis in insect cells are studied.
- >The Cu(II)-Allo9A complex at pH 7.4 displayed the highest haemocytotoxic activity.

ACCEPTED MANUSCRIPT